Specificity of the zebrafish host transcriptome response to acute and chronic mycobacterial infection and the role of innate and adaptive immune components

Sar, A.M. van der; Spaink, H.P.; Zakrzewska, A.; Bitter, W.; Meijer, A.H.

Molecular Immunology 46 (2009) 2317–2332

Contents lists available at ScienceDirect

Molecular Immunology

journal homepage: www.elsevier.com/locate/molimm

Specificity of the zebrafish host transcriptome response to acute and chronic mycobacterial infection and the role of innate and adaptive immune components

Astrid M. van der Sar[a], Herman P. Spaink[b], Anna Zakrzewska[b], Wilbert Bitter[a], Annemarie H. Meijer[b,*]

[a] Department of Medical Microbiology and Infection Control, VU University Medical Center, 1081 BT Amsterdam, The Netherlands
[b] Institute of Biology, Leiden University, Einsteinweg 55, 2333 CC, Leiden, The Netherlands

ARTICLE INFO

Article history:
Received 23 March 2009
Accepted 28 March 2009
Available online 5 May 2009

Keywords:
Tuberculosis
Microarray
TLR
WNT
Matrix metalloproteinases
Small GTPase signaling
MHC class I

ABSTRACT

Pathogenic mycobacteria have the ability to survive within macrophages and persist inside granulomas. The complex host–pathogen interactions that determine the outcome of a mycobacterial infection process result in marked alterations of the host gene expression profile. Here we used the zebrafish model to investigate the specificity of the host response to infections with two mycobacterium strains that give distinct disease outcomes: an acute disease with early lethality or a chronic disease with granuloma formation, caused by *Mycobacterium marinum* strains Mma20 and E11, respectively. We performed a microarray study of different stages of disease progression in adult zebrafish and found that the acute and the chronic strains evoked partially overlapping host transcriptome signatures, despite that they induce profoundly different disease phenotypes. Both strains affected many signaling cascades, including WNT and TLR pathways. Interestingly, the strongest differences were observed at the initial stage of the disease. The immediate response to the acute strain was characterized by higher expression of genes encoding MHC class I proteins, matrix metalloproteinases, transcription factors, cytokines and other common immune response proteins. In contrast, small GTPase and histone gene groups showed higher expression in response to the chronic strain. We also found that nearly 1000 mycobacterium-responsive genes overlapped between the expression signatures of infected zebrafish adults and embryos at different stages of granuloma formation. Since adult zebrafish possess an adaptive immune system similar to mammals and zebrafish embryos rely solely on innate immunity, this overlap indicates a major contribution of the innate component of the immune system in the response to mycobacterial infection. Taken together, our comparison of the transcriptome responses involved in acute versus chronic infections and in the embryonic versus adult situation provides important new leads for investigating the mechanism of mycobacterial pathogenesis.

1. Introduction

Tuberculosis remains among the most threatening infectious diseases world-wide with approximately 1.6 million deaths each year (WHO, http://www.who.int/tb/publications). Around one-third of the world population is infected with *Mycobacterium tuberculosis*, the causative agent of tuberculosis, and an estimated 5–10% of these people will develop active disease sometime during their life. The outcome of an infection with mycobacteria depends on the complex interactions between the immune defenses of the host and a pathogen's capacity to subvert them. Pathogenic mycobacteria, like *M. tuberculosis*, have developed strategies to evade eradication by the immune system in order to persist for a long time inside macrophages (Manabe and Bishai, 2000; Stewart et al., 2003). The host's immune system reacts on the prolonged infection with the formation of granulomas, which are composed of several cell types including macrophages, neutrophils and lymphocytes. Granuloma formation is a hallmark of tuberculosis and a critical step in the pathogenesis of this disease (Flynn and Chan, 2003; Gordon et al., 1994).

Innate immunity provides an important early defense against *M. tuberculosis* and could be a crucial determinant of the ultimate outcome of the infection. The innate response is triggered by interactions between surface structures on mycobacteria and pattern recognition receptors on the cell, such as the Toll-like receptors (TLRs). To circumvent destruction in lysosomes mycobacteria manipulate the macrophage to prevent or delay phagosome-lysosomal fusion and maturation. As a result mycobacteria may reside inside immature phago-lysosomes (Russell, 2001) and even translocate to the cytosol (Stamm et al., 2003; van der Wel et al.,

* Corresponding author. Tel.: +31 71 5274927.
E-mail address: a.h.meijer@biology.leidenuniv.nl (A.H. Meijer).

0161-5890/$ – see front matter © 2009 Elsevier Ltd. All rights reserved.
doi:10.1016/j.molimm.2009.03.024

2007). Not all mycobacteria escape destruction, what results in activation of the adaptive immune system leading to interferon-gamma (IFN-γ) secretion by T helper type 1 (Th1) CD4+ lymphocytes. IFN-γ activates macrophages to express anti-microbial activity. Activation of CD4+ T-cells, recruitment of CD8+ T-cells to the site of infection and the production of pro-inflammatory cytokines all contribute to the maintenance of adaptive immunity. As a reaction mycobacteria have developed strategies to modulate adaptive immunity towards a Th2 response leading to secretion of anti-inflammatory cytokines and suppression of adaptive immunity (Flynn and Chan, 2003).

Knowledge of specific molecules or pathways targeted by mycobacteria for immune evasion may provide insights into host–pathogen interactions that determine the outcome of infection. Pathogen-induced changes in host cells are generally accompanied by marked changes in gene expression due to host- and pathogen-mediated reprogramming of the transcriptome during infection (Jenner and Young, 2005). Global expression profiling studies therefore may reveal transcriptional responses specific for mycobacterial diseases and thereby provide valuable leads for further investigation of the process of mycobacterial pathogenesis. Microarrays have recently been applied to study susceptibility to *M. tuberculosis* infection in mice (Marquis et al., 2008) and to report on the immune response of animal populations naturally infected with *Mycobacterium bovis* (Fernandez de Mera et al., 2008; Naranjo et al., 2006). Furthermore unique host gene expression signatures have been attributed to specific strains of *Mycobacterium avium* in studies of human macrophage infections (Blumenthal et al., 2005; Coussens et al., 2003; Jenner and Young, 2005).

Here we used the zebrafish as an animal model to investigate the host response to a mycobacterial infection. Zebrafish can be infected by a natural mycobacterial pathogen, *Mycobacterium marinum*, and it has been well documented that the zebrafish-*M. marinum* model recapitulates hallmark features of human tuberculosis (Clay et al., 2007; Lesley and Ramakrishnan, 2008; Swaim et al., 2006). A particular advantage of the zebrafish-mycobacterium model is that besides studies in adults, which possess an adaptive immune system similar as mammals, the innate component of the immune response can be studied in the embryo model. Importantly, it has been shown that innate immunity is sufficient for granuloma formation in zebrafish embryos (Davis et al., 2002). Previously we reported on the transcriptome response of adult zebrafish at the end stage of a chronic *M. marinum* infection and showed that mycobacterium-infected zebrafish express many homologs of human immune response genes and genes that have previously been implicated in the response to mycobacterial infection (Meijer et al., 2005). In the present work we extended those studies with the aim to identify transcriptional patterns associated with different stages of mycobacterial infections caused by two distinct *M. marinum* strains, Mma20 and E11 that, respectively, induce an acute disease or chronic tuberculosis (van der Sar et al., 2004). In addition, we compared for the first time the differentially expressed genes and pathways between embryonic and adult-infected zebrafish. This is of particular interest, since this allows for the dissection of gene regulation only by innate immunity in the case of embryonic infections, and gene regulation in the presence of full immunity in the case of adult infections (Davidson and Zon, 2004; Lam et al., 2004; Willett et al., 1999). For this study we developed a custom microarray enriched for zebrafish homologs of mammalian immune response genes that we identified by data mining of the zebrafish transcript and genome databases. The results of this study provide a genomic repository of mycobacterium-responsive genes at different stages of disease progression and contribute to the basic understanding of the mechanisms of pathogenesis, protective immunity and resistance to mycobacterial infections.

2. Materials and methods

2.1. Bacterial strains and growth conditions

M. marinum strains E11 and Mma20 have been described before (van der Sar et al., 2004). Bacteria were grown at 30 °C in Middlebrook 7H9 medium supplemented with Middlebrook oleic acid-albumin-dextrose-catalase (BD Biosciences) and 0.05% Tween-80. Prior to inoculation in zebrafish, bacteria were washed in phosphate-buffered saline (PBS) and 0.3% Tween-80 and diluted in PBS. Bacterial numbers were determined by measuring the optical density at 600 nm and by plating and CFU determination.

2.2. Zebrafish husbandry and infection experiments

Zebrafish were handled in compliance with the local animal welfare regulations and maintained according to standard protocols (http://ZFIN.org). Infection experiments were approved by the local animal welfare committee (DEC) of the VU University medical center and of Leiden University. Infection experiments with adult fish were performed on young males selected from a wild type laboratory-breeding colony and acclimated to their new environment for one week in a quarantine area. These fish were kept at 28 °C on a 12:12 h light/dark rhythm throughout the experiment. Groups of 10 fish, infected with the same dose and strain of mycobacteria, were kept in small fish tanks (10 l) with their own separate filtering system (Eheim Ecco). Zebrafish were inoculated intraperitoneally as previously described (van der Sar et al., 2004) with approximately 10^4 bacteria or with phosphate-buffered saline (PBS) as a control. For the acute infection study with E11 and Mma20 strains, 3 fish per group were sacrificed at 1 and 6 days post infection (dpi) and used for microarray analysis. For comparison with the end stage of chronic E11 infection we used RNA samples from our previously published chronic infection study ((Meijer et al., 2005); control fish c2 and infected fish i2) and additional RNA samples (2 controls, 2 infected) from a similar infection experiment. All chronically infected fish showed overt signs of fish tuberculosis, including lethargy and skin ulcers. Histological examination of fish from the same experiments confirmed that the pathology of infected fish corresponded to fish tuberculosis (van der Sar et al., 2004) and that no characteristics of the disease were present in the control fish.

Infection experiments at the embryonic stage were performed using mixed egg clutches from different pairs of AB strain zebrafish. Embryos were grown at 28.5–30 °C in egg water (60 μg/ml Instant Ocean see salts) and for the duration of bacterial injections embryos were kept under anaesthesia in egg water containing 0.02% buffered 3-aminobenzoic acid ethyl ester (tricaine, Sigma). Embryos were staged at 28 h post fertilization (hpf) by morphological criteria (Kimmel et al., 1995) and approximately 50 cfu of E11 bacteria were injected into the caudal vein close to the urogenital opening. As a control an equal volume of PBS was likewise injected. Infection experiments were carried out in triplicate on separate days and pools of 25–30 embryos were taken at 2, 24 and 120 h post infection (hpi).

2.3. RNA isolation, labeling and hybridization

Adult fish and embryos for RNA isolation were snap frozen in liquid nitrogen and subsequently stored at −80 °C. Adult fish were homogenized in liquid nitrogen using a mortar and pestle and portions of 50–100 μg of powdered tissue were used for extraction of total RNA with 1 ml of TRIZOL® Reagent (Invitrogen) according to the manufacturer's instructions. Embryos were directly homogenized in TRIZOL® Reagent. The RNA samples were incubated for 20 min at 37° with 10 units of DNaseI (Roche Applied Science) to remove residual genomic DNA prior to purification using the

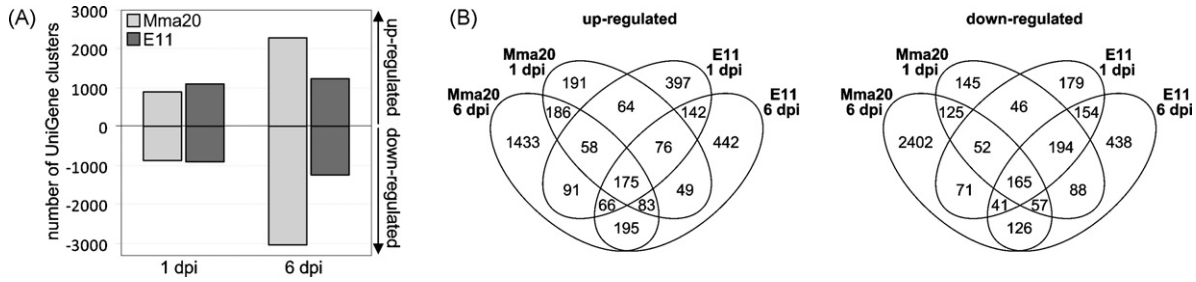

Fig. 1. Early response of adult zebrafish to infection with *M. marinum* strains Mma20 and E11. (A) Number of UniGene clusters up- and down-regulated (≥1.5 absolute fold change, $P \leq 10^{-4}$) by Mma20 and E11 infection at 1 and 6 dpi. (B) Venn diagrams showing the overlap of UniGene clusters up-regulated and down-regulated by the different strains and at the different time points.

RNeasy MinElute Cleanup kit (Qiagen) according to the RNA clean up protocol. The integrity of the RNA was confirmed by Lab-on-chip analysis using the 2100 Bioanalyzer (Agilent Technologies). Samples used for microarray analysis had an average RIN value of 9 and a minimum RIN value of 8.

Amino Allyl modified aRNA was synthesized in one amplification round from 1 μg of total RNA using the Amino Allyl MessageAmp™ II aRNA Amplification Kit (Ambion). Subsequently, 6 μg of Amino Allyl modified aRNA was used for coupling of monoreactive Cy3 and Cy5 dyes (GE Healthcare) and column purified. All samples of the early adult infection study (1 and 6 dpi infection with Mma20 and E11 strains and PBS-injected controls) were labelled with Cy5 dye and hybridized against a Cy3-labelled common reference, consisting of a mixture of samples from the same experiment. All samples from the embryo infection study (2, 24 and 120 hpi infection with strain E11 and PBS-injected controls) were also labelled with Cy5 dye and hybridized against a Cy3-labelled common reference, consisting of a mixture of samples from embryo infections described in Stockhammer et al. (2009). For the chronic E11 infection study samples from infected fish were labelled with Cy5 dye and samples from PBS-injected control fish with Cy3 dye. The dual colour hybridization of the microarray chips was performed at ServiceXS (ServiceXS, Leiden, The Netherlands) according to Agilent protocol G4140-90050 v.5.7 (www.Agilent.com) for Two-Color Microarray-Based Gene Expression Analysis. The microarray slides were custom designed by Agilent Technologies as described in Stockhammer et al. (2009). The microarray design has been submitted to the Gene Expression Omnibus (GEO) database, under platform submission number GPL7735. All microarray data were submitted to the GEO database under series GSE15328.

2.4. Data analysis

Microarray data were processed from raw data image files with Feature Extraction Software 9.5.3 (Agilent Technologies). Processed data were subsequently imported into Rosetta Resolver 7.1 (Rosetta Biosoftware, Seattle, Washington) and subjected to default ratio error modeling. The Rosetta built-in re-ratio with common reference application was used to calculate ratios between infected and control samples for the early adult infection study (1 and 6 dpi) and for the embryo infection study. For the chronic E11 infection experiments, triplicate ratio results from control versus infected adult fish were combined using the default ratio experiment builder. Data were analyzed at the level of UniGene clusters (UniGene build #105). The significance cut-off for ratios of infected versus control was set at $P \leq 10^{-4}$. For adult infection studies, where triplicate individuals are tested, an absolute fold change cut-off (≥1.5) was applied additionally. For embryo infection studies, where triplicate pools of 25–30 individuals are tested, no fold change cut-off was applied. Differences between responses to the Mma20 and E11 strains and between acute and chronic E11 infection were analyzed by one-way ANOVA analysis (error-weighted) with Benjamin–Hochberg FDR multiple test correction. Only those UniGene clusters were included for which at least one of the ratio experiments met the thresholds of 1.5-fold change and $P \leq 10^{-4}$, and the significance cut-off for ANOVA testing was set at $P \leq 0.01$. Cluster analyses were performed with Rosetta Resolver settings for agglomerative algorithm (average link) with Pearson correlation (weight by error). Gene ontology (GO) analysis was performed with DAVID software tools for Functional Classification and Functional Annotation Clustering (http://david.abcc.ncifcrf.gov/home.jsp) (Dennis et al., 2003) with default settings and the *Danio rerio* Entrez Gene IDs as input.

3. Results

3.1. Microarray design and validation

In an earlier study we used Affymetrix, MWG and Sigma-Compugen microarray platforms to profile the zebrafish host transcriptome response at the late stage of *M. marinum* infection (Meijer et al., 2005). However, we noted that many immunity-related genes were not represented on these three microarray platforms. For the present study, we therefore switched to the more flexible Agilent platform and made a custom 44k design that includes Agilent's own 22k probe set released in 2005, a 16k set of probes similar to the Sigma-Compugen oligonucleotide library used in our previous study, and a 6k set of probes for selected genes of interest that we identified by data mining of zebrafish transcript and genome databases. Most of the genes of our custom array are represented by more than one probe, together accounting for a total of 19,122 different UniGene clusters. In the previous study we presented a reference set of differentially expressed genes detected by the Affymetrix, MWG and Sigma-Compugen platforms (Meijer et al., 2005). Here, we hybridized the same RNA samples to our new Agilent platform and could confirm differential expression of 94% of these genes with a *P*-value lower than 0.01 and of 87% with a *P*-value lower than 10^{-4} (Supplementary Table S1). Additionally, 6 differentially expressed genes previously validated by quantitative PCR analysis, were also confirmed by Agilent microarray analysis ($P \leq 10^{-4}$) (Supplementary Table S1).

3.2. Early response of adult zebrafish to infection with *M. marinum* strains Mma20 and E11

Previously we showed that *M. marinum* strains can be divided into two distinct clusters based on genetic diversity and virulence (van der Sar et al., 2004). Here we compared the adult zebrafish host transcriptome responses towards early infection with strain Mma20, a representative from cluster I that causes an acute disease phenotype, and strain E11, a representative from cluster II that causes a chronic disease phenotype. Fish were sampled for microar-

ray analysis at 1 and 6 dpi with 3 biological replicates per group. In agreement with previous observations, the fish infected with Mma20 began to show acute disease symptoms like a swollen belly at 6 dpi, while the appearance of fish infected with E11 was normal at this stage. The acute disease state of the 6 dpi Mma20 group was also apparent from our microarray analysis that identified more than 5000 up- or down-regulated UniGene clusters for this group, which was 2–3-fold more than for the other three groups (Mma20 1 dpi, E11 1 dpi, E11 6 dpi) (Fig. 1A).

First we determined the overlap in host genes induced or repressed by the different strains (Fig. 1B) and subjected the resulting gene lists (Supplementary Table S2) to Gene Ontology using DAVID software tools for Functional Classification and Functional Annotation Clustering (Dennis et al., 2003). These are complementary tools designed to identify functionally related gene groups that are significantly enriched with respect to the microarray background. DAVID analysis (Supplementary Table S3) indicated that at 1 dpi the Mma20 and E11 strains both caused up-regulation of 373 genes, including a group of around 50 genes involved in regulation of transcription, around 40 genes with the GO-term zinc-ion binding and around 10 genes associated with heme metabolic processes, including several cytochrome P450 genes. A group of 175 genes consistently up-regulated by both strains and at both time points contained at least 14 genes encoding zinc finger proteins, including kruppel-like factors and ring-fingers, at least 4 apoptosis-related genes, including *casp9* and *bad*, and a number of immune response-related transcription factor genes, including *cebpd*, *cebpg* and *fos*.

Gene groups that were down-regulated at 1 dpi by both the Mma20 and E11 strains had GO-terms related to ribosome biogenesis and assembly, protein metabolism, protein folding, ATP-binding and biosynthetic processes (457 genes in total). A group of 165 genes consistently down-regulated by both strains and at both time points also predominantly contained genes involved in metabolic processes. In addition, gene groups with the GO-term membrane attack complex appeared in all down-regulated gene lists. Interestingly, while transcriptional regulators were among the up-regulated gene groups at 1 dpi, they were among the down-regulated groups at 6 dpi (165 genes for Mma20, 31 genes for E11). A gene group encoding zinc-ion binding proteins (83 genes) was also down-regulated by Mma20 infection at 6 dpi, in contrast to its up-regulation by E11 at the same time point and by both Mma20 and E11 at 1 dpi. In addition, acute infection with the Mma20 strain was associated with down-regulation of developmental gene groups (nervous system, eye, muscle), and genes associated with negative regulation of signal transduction, G-protein-coupled receptor activity and transporter activity.

In conclusion, our data showed that Mma20 and E11 infections evoke partially overlapping host responses, despite that they cause profoundly different disease phenotypes. A particularly notable similarity was the initial up-regulation of transcription factor gene groups at 1 dpi and their subsequent down-regulation when the infections progressed.

3.3. Statistical analysis of differences in the initial host response to Mma20 and E11 infection

To identify specific differences between the effects of the Mma20 and E11 strains on the host immune response, the 1 dpi time point was most relevant, given the acute disease symptoms caused by the Mma20 strain at 6 dpi. We therefore subjected the 1 dpi data sets to a one-way ANOVA analysis with Benjamin–Hochberg FDR multiple test correction. A total of 835 UniGene clusters were found to be differentially regulated between the two strains (Supplementary Table S4). In order to visualize the behavior of these genes over all time points we performed a 2D agglomerative cluster analysis (Fig. 2). In the first dimension, the two strains rather than the time points clustered separately, indicating that the majority of strain-specific differences detected at 1 dpi extended through to 6 dpi. In the second dimension, two main subclusters were identified, one with genes showing higher expression with Mma20 infection than with E11 infection (Mma20 > E11) and one with genes showing lower expression with Mma20 infection than with E11 infection (Mma20 < E11) (Supplementary Table S4).

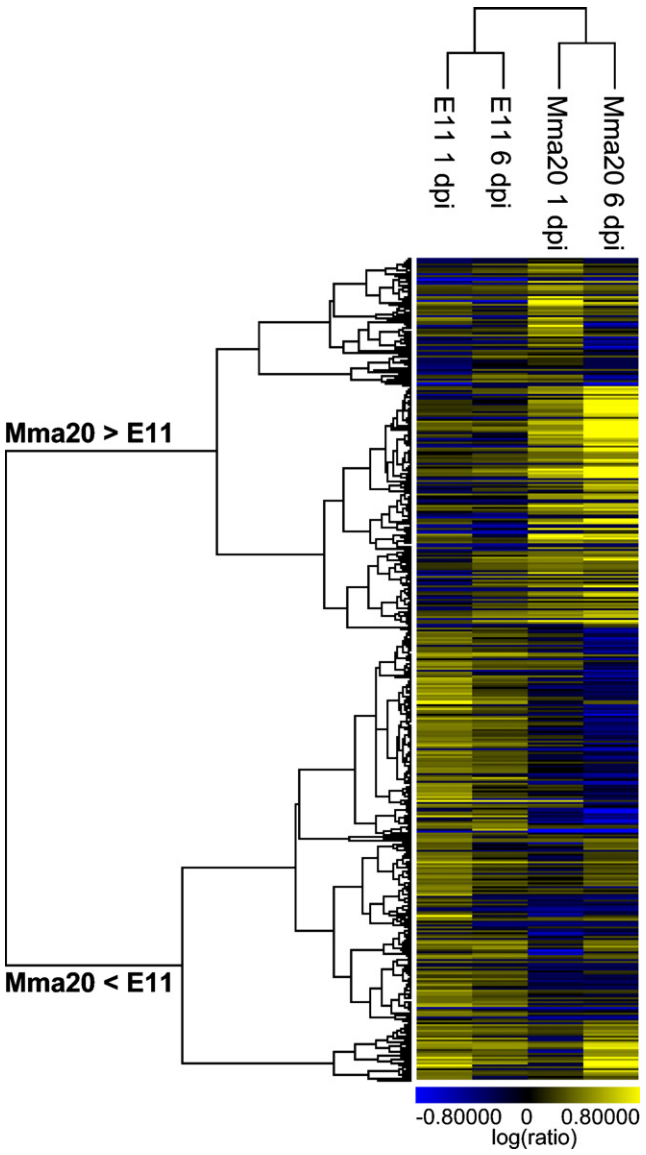

Fig. 2. 2D-cluster analysis of a group of 835 genes showing differential expression between the Mma20 and E11 strains at 1 dpi based on one-way ANOVA statistical testing ($P \leq 0.01$). Ratio experiments used for clustering included the 1 and 6 dpi time points of both strains. Two main subclusters are designated as Mma20 > E11 and Mma20 < E11.

The Mma20 > E11 subcluster appeared to be specifically enriched for four gene groups with the GO-terms, regulation of transcription, response to stimulus, extracellular region, and antigen presentation via MHC class I (Table 1, and Supplementary Table S4 for the supporting gene lists with fold changes and *P*-values). The majority of genes in the regulation of transcription group (26 out of 29) were up-regulated by Mma20 infection, while unresponsive or up-regulated to a lower extent by E11 infection. This group includes genes encoding transcription factors of the Irf, Jun/Fos, Atf,

Table 1
Gene Ontology (GO) analysis of genes responding differentially to *M. marinum* Mma20 and E11 infection at 1 dpi.

	Mma20 > E11			Mma20 < E11			Genes in group
	Count	Size	Score	Count	Size	Score	
Gene Functional Classification							
BP_regulation of transcription	29	29	1.34				tbx6, ascl1b, bzw1, zgc:77060, foxi3b, irf11, fos, mycb, hoxa13b, maf, wu:fk63e10, homez, zgc:85969, tsc22d3, rel, junbl, jun, irf8, reverbb1, zgc:92106, cebpb, atf3, cebpd, nfkb2, junbl, zgc:66473, zgc:85857, nr1d1, si:ch211-238e6.5
BP_small GTPase-mediated signal transduction				10	10	1.71	zgc:92926 (Rab40 subfamily), rab5al (Rab5 subfamily), zgc:73061(Rab39 subfamily), zgc:110645 (Rab5 subfamily), zgc:101893 (RabL4 subfamily), rala (Ras subfamily), rnd1(Rnd1/Rho6 subfamily), zgc:64022 (RERG/RasL11-like subfamily), cdc42l2 (Cdc42 subfamily), zgc:92870 (Ras subfamily)
BP_chromatin assembly and disassembly				5	5	1.69	zgc:65861 (linker histone 1 and histone 5 domains), h2afvl (histone 2A family member ZA), h2afv (histone 2A family, member V), mid1ip1 (histone cluster 2, H2ab), zgc:63676 (histone cluster 1, H2ah)
Functional Annotation Clustering							
BP_cellular component organization and biogenesis				28	35	1.66	lgtn, h2afv, dzip1, pane1, zgc:112262, jmjd6, bnip3l2, zgc:123274, zgc:55580, tbx2b, eif4e1b, zgc:56330, agxt, zp3b, slc25a27, ctsl1b, tuba4l, wu:fj49c01, nr1i2, nrp1a, zgc:63676, zgc:55995, zgc:63736, rarga, zgc:66125, zgc:65861, ptk2.1, mid1ip1, robo2, nudt1, h2afvl, tube1, cat, sema3ab, esr1
BP_immune system development				5	7	1.34	zgc:109721, si:busm1-194e12.11, stat5.1, bmp4, ba2, melk, nrp1a
BP_response to stimulus	26	28	4.05				igfbp-1, tlr 5a, tnfb, gadd45b, hyou1, il1b, cxcr4b, zgc:111997, tlr21, tnfa, opn1mw1, zgc:152866, mxc, mhc1uea, ptgs2a, mhc1uda, hamp1, jun, ifng1-2, atf3, dap3, stm, or115-10, cyp2k6, cfb, tpsn, mhc1ufa, tlr22
BP_antigen presentation via MHC class I	5	5	1.70				mhc1uea, mhc1uda, zgc:111997 (mhc class I family), mhc1ufa, tpsn (mhc class I family)
CC_extracellular region	10	15	2.19				zgc:85866, hamp1, igfbp-1, tnfb, ifng1-2, tnc, atf3, hyou1, zgc:77076, il1b, mmp9, tnfa, cfb, mmp13, mxc

Differences between responses to the Mma20 and E11 strains at 1 dpi were analyzed by one-way ANOVA analysis and the resulting genes were subjected to cluster analysis as shown in Fig. 1C. Genes in the two subclusters, Mma20 > E11 and Mma20 < E11 were subjected to GO analysis with DAVID tools (Dennis et al., 2003). The Functional Classification tool reduces gene lists into functionally related gene groups. Functional Annotation Clustering is a complementary tool that groups GO-terms with similar biological meaning together using a grouping algorithm that is based on the hypothesis that similar annotations should have similar gene members. Both tools rank the importance of the discovered gene groups according to EASE enrichment score, which is the minus log transformation of the geometric mean of *P*-values from the enriched annotation terms associated with the different gene group members. Only groups with EASE scores larger than or equal to 1.3 were considered (geometric mean of *P*-values ≤ 0.05). For each group a representative GO-term for Biological Process (BP) or Cellular Component (CC) was selected. The table lists the total number of genes in each group (size), the number of genes in that group associated with the selected GO-term (count) and the EASE enrichment score. Note that some genes are assigned to more than one gene group.

Cebp, and NF-κb families. Likewise, most genes in the response to stimulus group (21 out 28) were up-regulated by Mma20 infection to a higher extent than by E11 infection. This group includes cytokine and interferon genes (*tnfa*, *tnfb*, *il1b*, *infg1-2*), toll-like and chemokine receptor genes (*tlr5a*, *tlr5b*, *tlr22*, *cxcr4b*), and other common immune response genes, such as those involved in the complement reaction (*cfb*), prostaglandin synthesis (*ptgs2a*), and the antimicrobial response (the hepcidin gene *hamp1*). The extracellular region group shows much overlap with the response to stimulus group, but unique members are the matrix metalloproteinase genes *mmp9* and *mmp13*. Notably, at 6 dpi both *mmp* genes were also differentially regulated, with, respectively, 41- and 13-fold higher up-regulation of *mmp9* and *mmp13* by Mma20 infection (Supplementary table S4). Finally, the antigen presentation via MHC class I group contains 3 genes that were very strongly up-regulated by Mma20 infection (*mhc1uea*: 497-fold; *mhc1uda*: 2 UniGene clusters, 239- and 32-fold; *mhc1ufa*: 196-fold) but down-regulated by E11 infection (*mhc1uea*: 8.6-fold; *mhc1uda*: 2 UniGene clusters, 2.5- and 4.1-fold; *mhc1ufa*: 3.2-fold). The strong up-regulation of these genes by Mma20 infection was a temporary effect, since they were down-regulated at 6 dpi with both strains. In addition, the antigen presentation group contains one MHC I gene that was unresponsive to Mma20 infection and strongly down-regulated by E11 infection (*zgc:111997*) at both 1 and 6 dpi (79- and 93-fold, respectively).

The Mma20 < E11 subcluster was enriched for four gene groups with the GO-terms, small GTPase-mediated signal transduction, chromatin assembly and disassembly, cellular component organization and biogenesis, and immune system development (Table 1, and Supplementary Table S4 for the supporting gene lists with fold changes and *P*-values). The small GTPase group consists of ten members with representatives from the Rab, Ras, Rho, Rnd and Cdc42 subfamilies. Five of these were down-regulated by Mma20 infection and less down-regulated or unresponsive to E11 infection (*rab5al*, *zgc:73061*, *zgc:101893*, *rala*, *rnd1*), four were not significantly responsive to Mma20 but up-regulated by E11 (*zgc:110645*, *zgc:64022*, *cdc42l2*, *zgc:92870*), and one was up-regulated by both strains but stronger by E11 (*zgc:92926*). For most of the small GTPase genes (8 out of 10) the differential response to Mma20 and E11 infection was an early effect observed at 1 dpi only. In two cases (*zgc:92926*, *zgc:101893*) the observed difference was persistent at 6 dpi. The chromatin assembly and disassembly group contained five histone gene family members. Three of these were not significantly responsive or slightly up-regulated by Mma20 infection and up-regulated to a higher extent by E11 infection. The other two were down-regulated by Mma20 infection and unresponsive or less down-regulated by E11 infection. In all cases differential regulation of histone genes was an early effect observed at 1 dpi only. The five histone genes were also present in the cellular component organization and biogenesis group, which additionally contained

a rather mixed set of genes with functions in diverse cellular processes. Finally, the immune system development group contained the *si:busm1-194e12.11* gene encoding MHC II class alpha domain protein, which was 17- and 20-fold down-regulated by Mma20 infection at 1 and 6 dpi, respectively, while not significantly responsive to E11 infection.

Taken together our data show that, besides a substantial degree of overlap, significant differences exist in the initial host responses to infections with identical doses of the acute disease causing Mma20 strain and the chronic disease causing E11 strain. Specifically, the response to the acute strain was characterized by higher expression of genes encoding MHC class I proteins, matrix metalloproteinases, transcription factors, cytokines and other common immune response proteins. In contrast, small GTPase and histone gene groups showed lower expression in response to the acute strain.

3.4. Comparison of the end stages of Mma20 and E11 infection

While Mma20-infected fish become symptomatic and start dying within a week after infection, zebrafish inoculated with the E11 strain commonly do not show external signs of disease until 6–8 weeks after the infection when clear symptoms, such as skin ulcers, a swollen belly and moribund behavior, suddenly manifest. Microarray analysis of the end stage of E11 infection showed that a total of 2079 UniGene IDs were up-regulated and 2872 were down-regulated (Supplementary Table S5). We subjected this data set to a 2D-cluster analysis together with the above-described data sets of Mma20 and E11 infections at 1 and 6 dpi. 2D-cluster analysis revealed a higher similarity between the end stages of E11 and Mma20 infection than between the early and end stages of E11 infection (Fig. 3). A total of 963 up-regulated and 1268 down-regulated UniGene IDs were overlapping between the data sets of the E11 and Mma20 end stages (Supplementary Table S5). The overlap group of up-regulated genes contained several immunity-related transcription factor genes (e.g. *atf3*, *cebp1*, *cebpa*, *cebpb*, *cebpd*, *hhex, hif1al, junb, junbl, pea3*, *nfkb2*, *rel*, *spi1*) as well as several genes involved in toll-like receptor signaling (*tlr1, tlr2*, *tlr5a*, *tlr5b*, *tlr8b*, *tlr22*, *myd88*, *tirap*, *irak4*). Other examples include cytokine genes (*il1b*, *il10*, *tnfa*, *tnfb*), chemokine receptor genes (*cxcr4b*, *cxcr3.2*), complement component genes (*c3b*, *c6, cfb*), matrix metalloproteinase genes (*mmp9*, *mmp13*, *mmp14a*) and a group of at least 13 lysosomal proton transporter genes. Also notable was that the overlap group contained several up-regulated genes with the GO-terms GTP-binding or small GTPase-mediated signal transduction, including those encoding guanyl-nucleotide exchange factors (GEFs, 7 family members), Ras GTPases (*rab7*, *rhogb*, *rhof*) and G-protein alpha inhibitors (*gnai1*, *gnai2*, *gnai2l*). Examples of down-regulated genes in the overlap group include genes encoding various types of metabolic proteins, solute carriers (9), crystallins (5), intermediate filament proteins (10) and connexins (4). In addition, this group includes 6 distal-less homeobox genes, 6 *hox* cluster genes and the *nitr9* gene. We also noted that several genes involved in WNT signaling were up- or down-regulated at the end stages of both Mma20 and E11 infection. To visualize the effects on this pathway we projected the microarray data onto a GenMAPP pathway (Fig. 4). As shown in the WNT pathway (Fig. 4A), the expression of several *wnt* genes, Wnt inhibitor genes and Wnt receptor genes (*fzd* family) was down-regulated by both strains. However, *wnt5a* expression was up-regulated by both strains.

ANOVA statistical testing showed that a total of 3625 UniGene IDs showed significantly different expression between the end stages of Mma20 and E11 infection. We removed all UniGene clusters that showed more than 1.5-fold change in the same direction, thus narrowing down the list to 1430 UniGene IDs that were specifically responsive to the E11 end stage (700 up, 730 down) and 1537

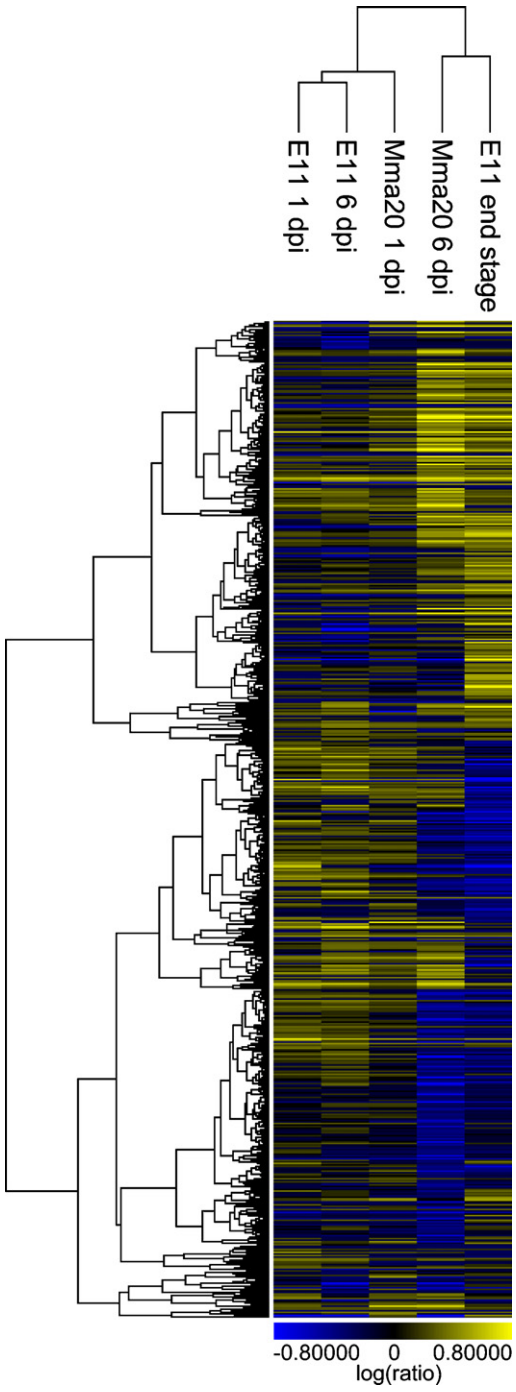

Fig. 3. 2D-cluster analysis of genes responsive to the early and end stages of Mma20 and E11 infection. Ratio experiments used for clustering included the 1 and 6 dpi time points of the early Mma20 and E11 infection study and the end stage point of the chronic E11 infection study. Only those UniGene IDs were included for which at least one of the ratio experiments met the thresholds of absolute fold change $\geq$1.5 and $P \leq 10^{-4}$.

UniGene IDs (614 up, 923 down) that were specifically responsive to the Mma20 end stage (6 dpi) (Supplementary Table S5). Enriched gene groups specifically regulated by either the E11 or the Mma20 strain are shown in Table 2. Notably, a group of transmembrane receptors (including 9 G-protein coupled receptor genes, *tlr9*, and *tlr18*) was specifically up-regulated by the E11 strain. On the other hand, the Mma20 strain specifically up-regulated groups of genes involved in proteolysis (encoding peptidases and peptidase inhibitors), in cell cycle regulation (mitosis), actin polymerization

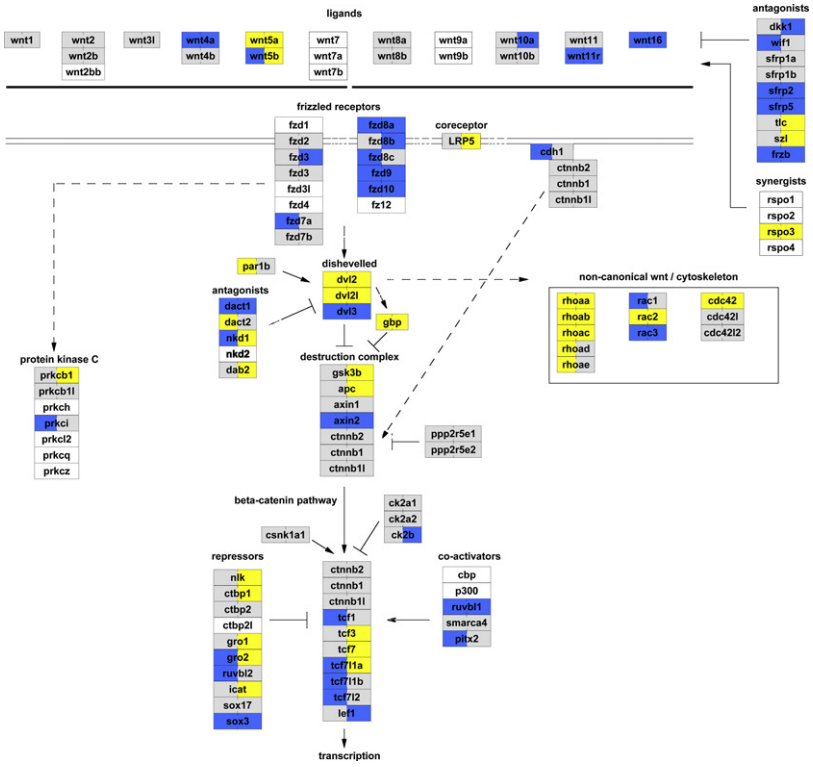

Fig. 4. Effects of Mma20 and E11 end stage infection on WNT signaling. Microarray data of E11-infected fish (end stage at 6–8 weeks) and Mma20-infected fish (end stage at 6 dpi) were projected onto the WNT signaling pathway using the GenMAPP program (www.genmapp.org) with $P \leq 0.001$ as significance cut-off. The canonical WNT GenMAPP was adapted from Krens et al. (2008). It should be noted that not all interactions have been experimentally confirmed in zebrafish. The left part of each gene box is colour coded with the Mma20 expression data and the right part with the E11 expression data. Up-regulation is indicated in yellow, down-regulation in blue and unchanged expression in grey. White denotes genes that were not represented on the array platform (For interpretation of the references to colour in this figure legend, the reader is referred to the web version of the article.).

(encoding arp2/3 complex subunits), and a group of genes involved in the response to biotic stimulus (including *mxb*, *mxc*, *hsp8*, *hsp90β*, *infg1-2*). Five *nitr* genes were specifically down-regulated at the E11 end stage (*nitr1c*, *nitr1i*, *nitr1o*, *nitr3a*, *nitr6b*). The Mma20 strain specifically down-regulated a group of 65 transcription factors, including 9 *hox* cluster genes and several other homeobox genes. Mma20 also down-regulated genes associated with the GO-term nervous system development (27) and the GO-term receptor binding (18), including 7 members associated with (neuro)peptide hormone activity.

In conclusion, our microarray studies of *M. marinum* infection in adult zebrafish indicate that overlapping as well as distinct host gene expression signatures are evoked by the E11 and Mma20 strains, both at the initial and at the end stages of the infection process.

3.5. E11 infection of zebrafish embryos

In contrast to adults, zebrafish embryos rely solely on innate immunity during the first days to weeks of their development (Davidson and Zon, 2004; Lam et al., 2004; Willett et al., 1999). However, similar to adults, embryos respond to *M. marinum* infection by the formation of granuloma-like aggregates (Fig. 5A). Here, we analyzed the host response of embryos at 2, 24 and 120 h post infection (hpi). As shown in Fig. 5B the number of up-regulated UniGene clusters peaked at 24 hpi, while the number of down-regulated UniGene clusters increased until 120 hpi. The overlap of up- and down-regulated UniGene clusters between the time points was fairly limited (Fig. 5C), which may be explained by the different stages of the infection process reflected at each time point (from initial response to granuloma formation). Furthermore, different competencies of the embryo's developing immune system are likely to play a role. In fact, at the start of the infection study the immune system consists primarily of primitive macrophages, at 24 hpi definitive hematopoiesis has begun and functional granulocytes have developed, and at 120 hpi the first immature lymphoblasts have formed and immune cells have seeded the thymus and head kidney (Herbomel et al., 1999, 2001; Lam et al., 2004; Murayama et al., 2006). Despite these differences, a few notable genes were up-regulated at all three time points, for example the small GTPase gene *rhobtb2a* and the zinc finger type transcription factor gene *plag2l*, whose homolog in mouse has been described as a leukemia oncogene that acts by expanding hematopoietic progenitor cells (Castilla et al., 2004; Landrette et al., 2005). Also *wnt4a* was up-regulated over all time points, however, GenMAPP analysis of the WNT pathway showed only limited regulation of other components of WNT signaling in embryos (Supplementary Figure S1). In addition to these specific genes, we observed that particular classes of genes were regulated over all time points, for example *hox* cluster genes (2 hpi: 12 down; 24 hpi: 6 up, 1 down; 120 hpi: 8 up, 5 down), and solute carrier genes (2 hpi: 5 up, 1 down; 24 hpi: 11 up, 8 down; 120 hpi: 2 up, 16 down).

Gene ontology analysis using DAVID tools (Table 3 and Supplementary Table 6 for the corresponding gene lists) showed that the set of UniGene clusters up-regulated at 2 hpi was enriched for a group of small GTPase genes, encoding 6 Ras and 3 Arf family members. A gene group associated with the GO-term ATP-binding, including 12 protein kinase genes, was also enriched. A group of 35 transcription factor genes was enriched among the down-regulated set at 2 hpi, notably including 12 *hox* cluster genes and several immune-related transcription factor genes that we found

Table 2
Gene groups with overlapping or differential responses during the end stages of *M. marinum* E11 and Mma20 infection.

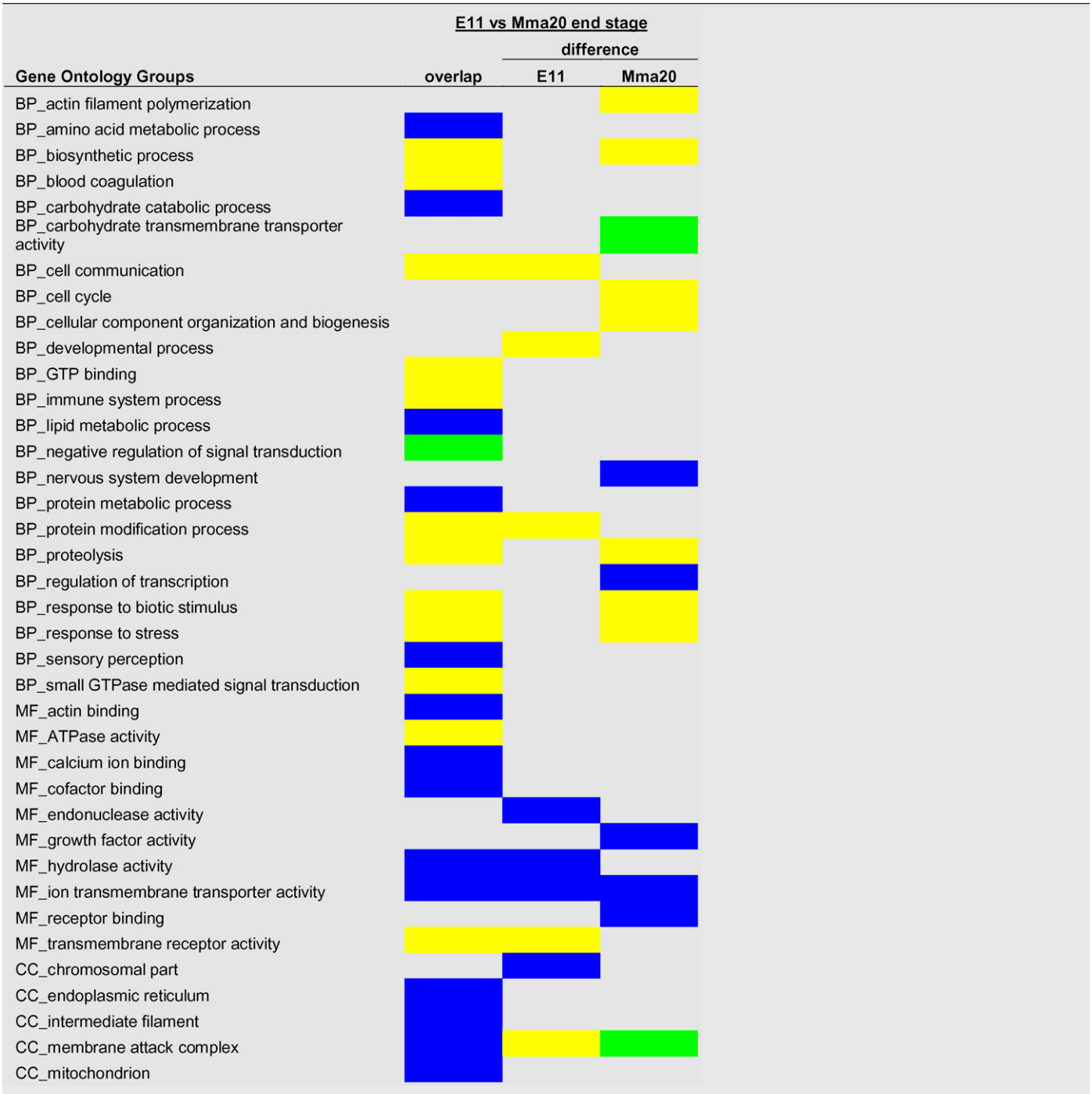

Gene ontology groups were determined using DAVID Functional Classification and Functional Annotation Clustering tools as in Table 1. For each group a representative GO-term for Biological Process (BP), Molecular Function (MF), or Cellular Component (CC) was selected. Some redundant gene groups were omitted from the table. The overlap column shows the enriched gene groups with ≥1.5 absolute fold change ($P \leq 10^{-4}$) at the end stages of both E11 (8 weeks) and Mma20 (6 days) infection. The difference columns show the enriched gene groups that were up- or down-regulated by E11 or Mma20 infection only, based on one-way ANOVA statistical testing. The input gene lists for DAVID analyses are given in Supplementary Table S5. Yellow boxes indicate up-regulated gene groups, blue boxes indicate down-regulated gene groups, and green boxes indicate gene groups consisting of both up- and down-regulated members.

up-regulated during infection of adult fish (*cebpb*, *cebpd*, *jun*, *junbl*, *rel*) and in some cases also at later stages of embryonic infection (*jun*, *rel*). In addition, a group of 4 cryptochrome genes (GO-term: photolyase activity) was enriched among the down-regulated genes at 2 hpi. Worth mentioning is also the up-regulation of *tlr1*, *tirap* and *stat3*, and the down-regulation of complement factor genes (*c3c*, *cfb*), lectin genes (*lgals3bp*, *lgals3l*) and *mhc1uea* at 2 hpi.

The main up-regulated gene groups that were enriched at 24 hpi were associated with regulation of transcription (72 genes, e.g. *atf7a*, *atf7b*, *dlx1a*, *dlx4b*, *gata4*, *gata5*, *gata6*, *hhex*, *jun*, *junb*, *pea3*), zinc-ion binding (41 genes), and translation (18, including 11 ribosomal protein genes). Several genes involved in WNT signaling (*wnt2*, *wnt4a*, *wnt4b*, *dkk1*, *dvl2*), BMP signaling (*bmp1a*, *bmpr2b*, *chd*, *grem1*), FGF signaling (fgf20a, fgf23, fgf24, fgfr1), and TLR signaling (*tlr1*, *tlr2*, *tlr19*) were also up-regulated. The main

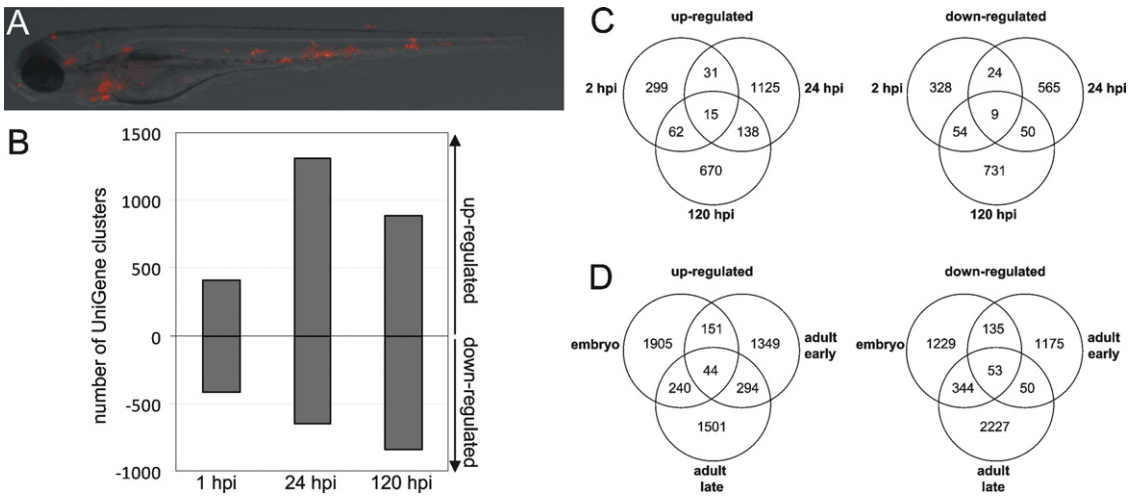

Fig. 5. Response of zebrafish embryos to infection with *M. marinum* strain E11. (A) Overlay of bright field and fluorescence images of an embryo infected with 50 cfu of DsRed-labelled E11 bacteria at 120 hpi. Granuloma-like aggregates are visible as red fluorescent clusters. (B) Number of UniGene clusters up- and down-regulated ($P \leq 10^{-4}$) at 2, 24 and 120 hpi. (C) Venn diagrams showing the overlap of UniGene clusters up-regulated and down-regulated at the different time points of embryo infection. (D) Venn diagrams showing the overlap of up- and down-regulated UniGene clusters identified in the embryo infection study (2, 24 and/or 120 hpi), the early adult infection study (1 and/or 6 dpi) and the chronic infection study (end stage) (For interpretation of the references to colour in this figure legend, the reader is referred to the web version of the article.).

Table 3
Gene groups regulated during *M. marinum* E11 infection of embryos.

Gene Ontology groups	2 hpi	24 hpi	120 hpi
BP_biological regulation			
BP_biosynthetic process			
BP_cell cycle			
BP_cell motility			
BP_cell surface receptor-linked signal transduction			
BP_embryonic development			
BP_gamete generation			
BP_inner ear development			
BP_multicellular organismal process			
BP_negative regulation of signal transduction			
BP_neuron development			
BP_protein modification process			
BP_regulation of transcription			
BP_response to chemical stimulus			
BP_response to stress			
BP_ribosome biogenesis and assembly			
BP_small GTPase-mediated signal transduction			
BP_translation			
BP_translational initiation			
BP_wnt receptor signaling pathway			
MF_ATP-binding			
MF_biopolymer metabolic process			
MF_DNA photolyase activity			
MF_GTP binding			
MF_ion transmembrane transporter activity			
MF_lipid binding			
MF_selenium binding			
MF_zinc ion binding			
CC_endoplasmic reticulum			
CC_membrane attack complex			
CC_ribosome			

Enriched gene ontology groups of the embryo infection study at 2, 24 and 120 hpi were determined using DAVID Functional Classification and Functional Annotation Clustering tools as in Tables 1 and 2. The input gene lists for DAVID analyses are given in Supplementary Table S6. Yellow boxes indicate up-regulated gene groups, blue boxes indicate down-regulated gene groups, and green boxes indicate gene groups consisting of both up- and down-regulated members.

down-regulated gene groups at 24 hpi were associated with the membrane attack complex (21 genes), ion transmembrane transporter activity (14), ATP-binding (14, of which 9 with hydrolase activity), and GTP-binding (12, including the Ras GTPases *rab5b*, *rab1a*, *rac1*, and *zgc:55558*).

At 120 hpi we observed up-regulation of gene groups associated with metabolic processes (178 genes), regulation of transcription (53 genes, e.g. *atf3*, *gro1*, *junb*, *rel*, *smad3b*, *stat5.2*), and protein modification (48 genes, of which 36 associated with kinase activity, e.g. *map2k3*, *mpa3k7*, *mos*, *mapk1*, *mapk3epha4a*, *epha4b*, *ek1*, *csf1r*, *src*, *jak2a*, *irak3*, and others with phosphatase activity, *ptpn11*, *ptpru*, *ptpra*). Additionally up-regulated were smaller gene groups associated with nervous system development (28), the cell cycle (18), and small GTPase-mediated signaling (10, including the Ras GTPases *rhobtb2a*, *rab30*, *rab32*, *rhoj*, *rnd1l*). As was observed for the up-regulated genes, transcription factor genes formed also an enriched group among the down-regulated genes (54, e.g. *cdx4*, *cebpd*, *dlx4a*, *gsc*, *hif1al*, *mef2a*, *mycn*, *snai1a*, *snai2*, *sox2*, *sox11b*, *sox17*). The main other down-regulated gene groups were associated with biosynthesis (43), the membrane attack complex (34), ribosome biogenesis and assembly (12), and negative regulation of signal transduction (11). Finally, some notable down-regulated genes at 120 hpi included complement factor genes (*bfb*, *c7*), membrane receptor genes (*cd36*, *cxcr4b*, *scarb1*), WNT signaling genes (*frzb*, *fzd8a*, *wnt4b*), and matrix metalloproteinase genes (*mmp9*, *mmp13*).

3.6. Overlap between adult and embryonic host responses to E11 infection

The overlap between the adult and embryonic host responses to E11 infection consisted of 435 up-regulated and 532 down-regulated UniGene clusters (Fig. 5D, Supplementary Table S7). In both cases transcription factor genes formed the largest functional group recognized by DAVID classification (23 up-regulated, 28 down-regulated). Up-regulated transcription factor genes that overlapped between adult and embryo included members of the atf (*atf3*, *atf7b*), ets (*ets1a*, *pea3*), jun (*jun*, *junb*), forkhead (*foxd5*, *foxk1*) and kruppel-like families (*klf11*, *klf2b*). Additionally, this group contained the *hhex* gene (hematopoietically expressed homeobox gene), which has been implicated in regulation of early endothelial and blood differentiation in zebrafish and has been suggested to be activated by WNT signaling (Liao et al., 2000; Bischof and Driever, 2004). Other genes that have been linked with hematopoiesis in zebrafish and that were up-regulated both in embryos and adults included *melk* and *spry4*, which are coding for a serine/threonine kinase and an inhibitor of map kinase signaling, respectively. The adult–embryo overlap group contained only a few cytokine genes (*il12a*, *tnfa*, *tnfb*), whereas several other cytokine genes were induced in adults (e.g. *il1b*, *il10*, *cxcl12a*). No matrix metalloproteinase genes of the *mmp* family were induced in E11-infected embryos, but the adult–embryo overlap group contained another metalloprotease gene, *adam8* (*CD156*), which is thought to play a role in a variety of biological processes involving cell–cell and cell–matrix interactions (Wolfsberg et al., 1995; Yamamoto et al., 1999). Other proteases in the overlap group included nothepsin (*nots*) and proteasome subunit genes (*psmb11*, *psmb3*). Some defense response genes up-regulated both in adults and embryos included those encoding hepcidin (*hamp1*), lysozyme C (*lyz*) and the p47 neutrophil NADPH oxidase subunit (*ncf1*), as well as genes involved in toll-like receptor signaling (*tlr1*, *tlr2*, *tirap*, *sarm1*). Finally, the gene encoding coronin (*coro1a*), which has been implicated in formation of the mycobacterial phagosome (Fratti et al., 2000; Kaul, 2008), was also up-regulated by E11 infection in both embryos and adults.

Down-regulated transcription factor genes that overlapped between adult and embryo included *gsc*, *mycn*, *otx5*, *prox1*, kruppel-like genes (*klf11* (also in up-regulated group), *klfd*), sox genes (*sox3*, *sox9a*, *sox11b*), and several types of homeobox genes (*cdx4*, *dlx3b*, *dlx4a*, *emx1*, *eng1a*, *hoxc12a*, *hoxc6a*). Examples of other genes down-regulated in both adults and embryos are those encoding apoptotic and/or proteolytic proteins (*caspb*, *cflar*, *psmd12*), lectins (*lgals3bp*, *lgals3l*), tight junction proteins (*cldn10l*, *cldnh*, *cldni*), and odorant receptors (*or103-2*, *or13.3*). Furthermore, several immune response genes were also down-regulated at certain stages of infection in both embryos and adults, for example *bfb* (complement family), *cd36* (scavenger receptor class B), *lect1* (encoding leukocyte cell derived chemotaxin 1), *mhc1uea* (MHC class I), *ptgds* (prostaglandin D2 synthase), *scarb1* (scavenger receptor class B), *tnfrsf21* (TNF receptor superfamily) and *trap1* (TNF receptor-

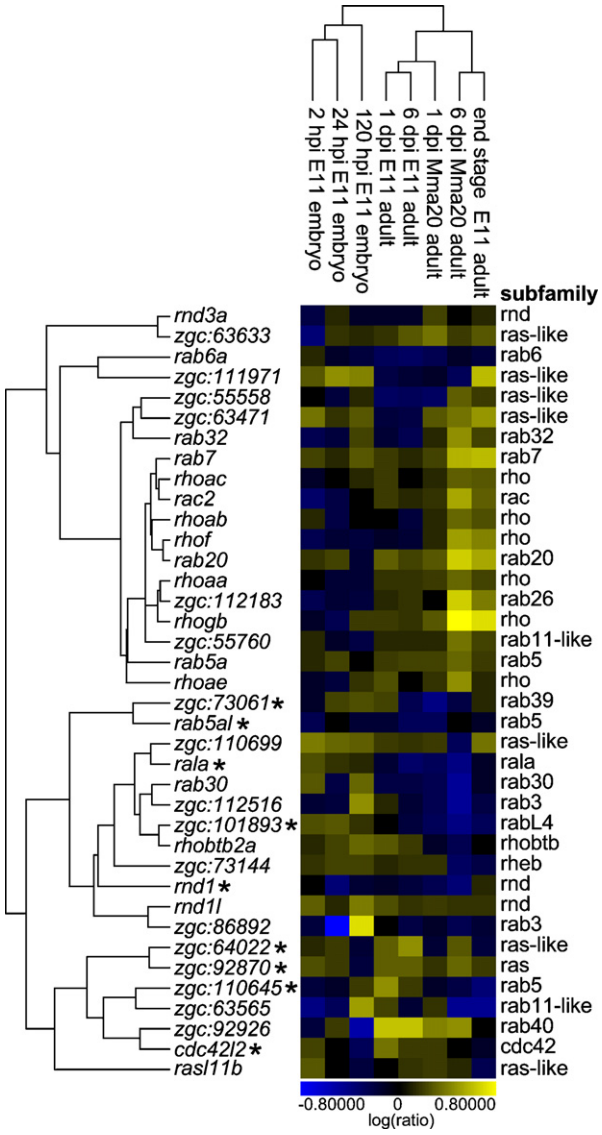

Fig. 6. Differential expression of small GTPases under different conditions of *M. marinum* infection. A 2D cluster analysis is shown of 38 genes for small GTPases that showed differential expression in at least one of the ratio experiments. Ratio experiments used for cluster analysis were of embryo infection by the E11 strain (2, 24, 120 h), early stages of adult infection by the E11 and Mma20 strain (1 and 6 dpi), and the end stage of E11 chronic infection (6–8 weeks). Note that fish at 6 dpi of Mma20 infection display similar end stage disease symptoms as the fish at the end stage of chronic E11 infection. Asterisks indicate GTPase genes showing significantly different expression between Mma20 and E11 infection at 1 dpi based on the ANOVA analysis. These genes fall in the Mma20 < E11 subcluster of Fig. 2.

associated protein 1). The overlap in expression signatures of embryos and adults indicates a major contribution of the innate component of the immune system in the response to *M. marinum* infection.

3.7. Regulation of small GTPase-mediated signaling during embryonic and adult infection

Genes involved in small GTPase-mediated signaling came out as an enriched group in several of the analyses described above. Altogether, a total of 38 small GTPases of the *ras/ral* (9), *rab* (16), *rnd* (3), *rheb* (1), *rho* (6), *rac* (1), *cdc42* (1) and *rhobtb* (1) subfamilies were differentially expressed under one or more tested conditions of *M. marinum* E11 and Mma20 infection. To visualize how the expression of these genes changed over the different experimental conditions we performed a 2D cluster analysis (Fig. 6). In the first dimension, the three embryo infection stages (2, 24, 120 hpi) clustered together. The same was true for the end stages of adult infection (6 dpi Mma20, 6–8 weeks E11) and the early stages of adult infection (1 and 6 dpi E11, 1 dpi Mma20). In the second dimension two main subclusters were apparent. The upper one was dominated by genes showing up-regulation at the end stages of adult infection, while the lower one contained genes with higher expression during embryonic infection and early stages of adult infection. All 6 rho GTPase genes were present in the upper subcluster, whereas *ras*-like and *rab* GTPase genes were spread over both subclusters. Several genes were up-regulated during embryo infection as well as during early and/or late stages of adult infection (e.g. *rab7*, *rab20*, *rnd1l*, *rhobtb2a*, and *ras*-like GTPases *zgc:63471*, *zgc:110699* and *zgc:92870*). In other cases the direction of change was different between embryo and adult infections (e.g. *rala* and the rab-like GTPases *zgc:101893*, *zgc:112516*). Finally, 2D cluster analysis supported the differential responsiveness of small GTPases to Mma20 and E11 infections. This was most evident in the lower subcluster, which contained nine GTPase genes that showed significantly different expression between Mma20 and E11 infection at 1 dpi based on the ANOVA analysis described above.

4. Discussion

Here we used the zebrafish as an animal model to delineate mechanisms involved in mycobacterial infection and disease progression reflected by changes in the host transcriptome. To identify transcriptional patterns associated with different stages of mycobacterial infection we compared transcriptome changes of adult zebrafish upon initial infection and after disease progression into either an acute or a chronic disease, caused by, respectively, *M. marinum* strain Mma20 or E11 (van der Sar et al., 2004). In addition, we used the E11 strain to profile the host response of zebrafish embryos prior to development of adaptive immunity. Our data show that a large set of mycobacterium-responsive genes (435 up-regulated and 532 down-regulated) overlapped between infected zebrafish adults and embryos at different stages of granuloma formation, indicative for a major contribution of the innate component of the immune system in the response to mycobacterial infection. We also observed strong similarities in the host response to Mma20 and E11 infections, particularly at the end stages of the resulting disease (963 up-regulated and 1268 down-regulated genes) but also immediately upon infection at 1 dpi (373 up-regulated and 457 down-regulated genes). Importantly, besides this common transcriptome response, our study revealed a set of 835 genes that responded differently to the Mma20 and E11 infections at 1 dpi. We analyzed this gene set for enrichment of specific gene ontology groups. Particularly notable was the higher expression of matrix metalloproteinases and MHC class I genes in the immediate response to infection with the acute strain (Mma20), in contrast to higher expression of small GTPase and histone gene groups in response to the chronic strain (E11). The relation of these gene groups to mycobacterial infection will be discussed below. Furthermore, we will reflect on how mycobacterial infection of zebrafish adults and embryos affected TLR and WNT pathways, two of the major signaling routes involved in the immune response.

4.1. Overlap and differences between Mma20 and E11 infections

Despite the clear difference in the type of infection induced by *M. marinum* Mma20 and E11, our microarray analyses revealed a substantial degree of overlap in the transcriptional responses to these strains. The responses upon initial infection (1 dpi) include up-regulation of gene groups with GO-terms related to regulation of transcription, zinc-ion binding, heme metabolic processes and apoptosis, and include down-regulation of the gene groups related to ribosome biogenesis and assembly, protein metabolism, protein folding, ATP-binding and biosynthetic processes. These overlapping responses reflect a common initial (transcriptional) reaction of the host upon pathogenic mycobacterial infection and fit well with transcriptome data of mycobacterium-infected cultured bovine or human cells and of bronchoalveolar lavage cells from tuberculosis patients (Blumenthal et al., 2005; Raju et al., 2008; Weiss et al., 2004). Furthermore, the induction of apoptotic genes is consistent with recent results of Davis and Ramakrishnan (2009) showing the role of apoptosis of infected macrophages in dissemination of *M. marinum* in zebrafish.

Pathological differences between the two strains become apparent when disease progresses. While zebrafish infected with *M. marinum* strain Mma20 manifest symptoms of acute disease after 6 days, fish infected with strain E11 display normal behavior. This difference in disease progression was correlated with a massive up- and down-regulation of transcripts at 6 dpi in Mma20-infected zebrafish compared with E11-infected zebrafish. For the chronic strain E11, there was much more similarity between the time points at 1 and 6 dpi. However, the transcriptome profile of the end stage of E11 infection, reached around 8 weeks post infection, was more comparable to that of the end stage of Mma 20. This observation indicates that, although E11 induces a chronic disease and subsequently needs more time to manifest itself, the biological processes that mark the end stage of mycobacterial infection are rather similar. Given this correlation between disease stage and transcriptome profile in both types of infection, the gene expression differences at the early stages of infection may provide important clues on key steps in mycobacterial disease progression. Below we focus on the transcriptional differences during the initial manifestation of the disease at 1 dpi that are likely to be most crucial for an acute or a chronic disease outcome.

4.2. Strongly induced tissue-remodeling transcripts

In general, already at 1 dpi, infection with Mma20 resulted in a stronger up-regulation of genes involved in antimicrobial responses than infection with E11. This is true for genes encoding inflammatory molecules like Tnfa and b, Infγ1 and 2, and Il1β, as well as for tissue-remodeling genes, such as *mmp9* and *mmp13*. Matrix metalloproteinases constitute a large family of Zn^{2+} dependent endopeptidases and maintain tissue allostasis by catalyzing the normal turnover of extracellular matrix macromolecules, proteoglycans and fibronectin. MMPs facilitate leukocyte recruitment, cytokine and chemokine processing and remodeling of matrix, and perform multiple roles in the normal immune response to infections (Goetzl et al., 1996; Parks et al., 2004). It has been shown for instance that MMP9 is responsible for the processing of cytokines, e.g. pro-IL1β and pro-TNFα,

into their active forms (Chang et al., 1996; Schonbeck et al., 1998).

Several studies reported on *MMP9* induction through mycobacterial stimulation *in vitro* or *in vivo* after infection with *M. tuberculosis*, *Mycobacterium leprae*, *M. bovis* BCG or *M. avium* (Basu et al., 2007; Elkington et al., 2007; Goetzl et al., 1996; Quiding-Jarbrink et al., 2001; Sheen et al., 2009; Taylor et al., 2006; Teles et al., 2007). Analysis of knockout mice with a pulmonary *M. tuberculosis* infection showed that *MMP9* expression is required for macrophage recruitment to the lungs and contributes to granuloma formation (Taylor et al., 2006). *MMP9* is induced during mycobacterial infections by TNFα, IL1β and TLR2 and suppressed by IL18, IFNs and progesterone (Birkedal-Hansen et al., 1993; Chang et al., 1996; Goetzl et al., 1996; Quiding-Jarbrink et al., 2001). In addition, it has been shown that induction of MMP9 by *M. avium* required NF-κB, histone acetyltransferase p300 and chromatin modifications (Basu et al., 2007). These studies indicate that MMP9 exerts multiple functions in mycobacterial infection and that activation of MMP9 is regulated on different levels and needs to be orchestrated well in time.

Although MMP9 clearly has a role in mycobacterial infection, the function of MMP13 is less well understood. Gonzalez-Avila et al. (2009) hypothesized that mycobacterial infections would have an effect on fibroblast collagen metabolism, since type I collagen synthesis and degradation are important events during granuloma formation. Indeed they showed an increase of *MMP13* mRNA levels and MMP13 pro-enzyme synthesis in fibroblasts incubated with *M. tuberculosis* H37Rv culture medium, suggesting that mycobacterial infection may have direct effects on fibroblast collagen turnover (Gonzalez-Avila et al., 2009). This is in line with the assumption that during chronic disease progression, mycobacteria contribute directly to granuloma and cavity formation via the stimulation of macrophages, T-cells and fibroblasts to release matrix metalloproteinases, resulting in collagen digestion. Indirectly, mycobacteria might contribute to granuloma formation by stimulating the release of TNFα and IL1β which in turn will induce release of matrix metalloproteinases and in addition will allow for leukocyte recruitment.

How might differences in *mmp9* and *mmp13* expression levels translate to the different disease progression of Mma20 and E11 infections in zebrafish? During infection with the Mma20 strain, rapid overstimulation of *mmp9/13* gene transcription may result in massive tissue damage. As shown in mice, this tissue destruction in the end causes host morbidity or mortality and favors pathogen dissemination (Taylor et al., 2006), a pathological stage identical to the end stage of Mma20 infection at day 6 post infection and to the end stage of E11 infection at 8 weeks post infection when *mmp* gene activity is also strongly induced. Also consistent with the results in mice (Taylor et al., 2006), a more moderate induction of *mmp* expression, as we observed during the early stages of infection with the E11 strain may contribute to granuloma formation and development of the chronic disease phenotype. Similarly, zebrafish embryos infected with *Salmonella typhimurium* displayed a massive increase in *mmp9* and *mmp13* transcripts much like Mma20-infected zebrafish (Stockhammer et al., 2009). These *S. typhimurium*-infected embryos succumbed quickly to the infection, while embryos infected with a non-pathogenic *S. typhimurium* Ra mutant strain showed a much lower increase in *mmp9* and *mmp13* expression (Stockhammer et al., 2009). Expression of *mmp9* and *mmp13* was not significantly increased during E11 infection of zebrafish embryos, indicating that the basal expression levels of these genes are sufficient for granuloma formation.

4.3. Antigen presentation via MHC class I

Mma20 infection resulted in a massive increase in gene expression of the MHC class I cluster (Table 1). In chronic mycobacterial infections in mammals, including humans, it has been shown that mycobacterial granulomas contain both CD4+ and CD8+ T-cells. For a long time researchers believed that pathogenic mycobacteria reside primarily in a membrane containing compartment, a view currently under debate (van der Wel et al., 2007). Based on this view, most attention was paid to the role of CD4+ T-cells and MHC class II presentation of mycobacterial antigens. Many studies have indeed confirmed the importance of CD4+ T-cells in mycobacterial infections (Caruso et al., 1999; Flynn and Chan, 2001; Muller et al., 1987; Orme and Collins, 1983). Only in recent years the importance of CD8+ T-cells and MHC I antigen presentation in mycobacterial infection and granuloma formation became apparent (Grotzke and Lewinsohn, 2005). Most of these studies focused on the role of CD8+ T-cells during persistent infection, from 1-week post infection onwards. Only after 2 weeks of infection an increase in the amount of mycobacterial activated CD8+ T-cells could be recovered from lungs of aerosol-infected mice (Serbina and Flynn, 1999). The early up-regulation of several MHC class I molecules (*mhc1uda*, *mhc1uea*, *mhc1ufa* and *tapasin*) in zebrafish infected with *M. marinum* strain Mma20 at 1 dpi is therefore remarkable. It is even more remarkable considering the fact that at 6 dpi there is a clear down-regulation of *mhc1* transcripts in Mma20-infected zebrafish. Infection with *M. marinum* strain E11 caused down-regulation of these MHC class I genes at early time points in adult infection (1 and 6 dpi) and also during embryonic infection at 2 hpi.

The coordinate expression of several MHC class I molecules in zebrafish suggests regulation by a common transcription factor, which itself may be differentially regulated during Mma20 and E11 infections. TNF and IFN mediate transcriptional regulation of MHC class I genes (Boehm et al., 1997; Drew et al., 1995; Goodbourn et al., 2000; Martin et al., 2007), but since TNF and IFN are up-regulated at 1 dpi as well as at 6 dpi, there are probably other regulators involved in this process. Recently interferon-regulatory factor 1 (IRF1) was reported to mediate transcriptional regulation of MHC class I genes in Atlantic salmon (Young et al., 2008) independent of IFN and IRF2 expression. The zebrafish *irf11* gene, closely related to *IRF1*, is also differentially transcribed in Mma20-infected zebrafish and might therefore account for the regulation of the MHC I genes. The differences in transcriptional regulation of MHC class I genes at 1 dpi indicate a clear difference in immunological response upon infection with *M. marinum* strains E11 and Mma20 and might help to predict the disease outcome. The ability of *M. marinum* strain E11 to suppress, already at early stages after infection, MHC class I expression and inhibit the development of acquired immunity might promote chronic infection.

4.4. Histone modification and chromatin remodeling

In addition to the above-mentioned transcriptional regulator mechanisms, histone modification and chromatin remodeling are possibly involved in mycobacterial infections. We observed that infection with the chronic disease inducing strain E11 led to higher expression levels of at least five members of the histone family compared to infection with the Mma20 strain (Table 1). In addition, histone deacetylase 9b was up-regulated at the end stages of infection with both strains. Histone deacetylation of specific promoter regions influences the expression level of the respective target genes. For example, histone deacetylation diminished the IFN gamma induced Human Leukocyte Antigen (HLA-DR) gene expression in human THP-1 monocytic cells upon mycobacterial infection (Wang et al., 2005). Furthermore, Pennini et al. (2006) found that chromatin remodeling at the MHC2TA gene, that regulates MHC class II expression, is a target of inhibition by *M. tuberculosis* (Pennini et al., 2006). Not only MHC class II but also MHC class I expression is regulated by histone modifications (Kotekar et al., 2008). Together these data indicate that regulatory mechanisms

via histone activation have profound effects on MHC expression in infected cells. Furthermore, increased DNaseI sensitivity and restriction enzyme accessibility indicated rapid remodeling of the *TLR2* promoter region following infection of macrophages with *M. avium* (Wang et al., 2002). Therefore regulation of chromatin structure might contribute to immune evasion by mycobacteria and the initial differences in histone gene expression that we observed upon Mma20 and E11 infections might play a role in determining the acute or chronic disease outcome.

4.5. Small GTPase gene expression

We found that many genes encoding small GTPases were transcriptionally regulated during mycobacterial infection. This is of great interest, since many bacterial pathogens are known to secrete proteins that manipulate host GTPase functions (Brumell and Scidmore, 2007; Lemonnier et al., 2007; Lerm et al., 2000). A cluster analysis of our transcription data indicated one group of GTPase genes that showed strong up-regulation at the end stages of Mma20 and E11 infection in adult fish. This group contained six members of the Rho GTPase family, including *rhogb*, for which we previously demonstrated mycobacterium-induced expression by RT-PCR analysis (Salas-Vidal et al., 2005). Rho GTPases, which are key regulators of intracellular actin dynamics, are downstream of many signaling cascades, including the non-canonical WNT signaling route discussed below. *M. avium* invasion was found to be dependent on the activation of Rho GTPases (Sangari et al., 2000). On the other hand, secretion of nucleoside diphophatase kinase, acting as a GTPase-activating protein, was suggested to aid *M. tuberculosis* pathogenesis by stimulating the conversion of Rho GTPases into their GDP-bound inactive form (Chopra et al., 2004). Furthermore, transgenic expression of a human Rho GDP dissociation inhibitor (D4-DGI) in mouse T-cells impaired granuloma formation by the *M. bovis* BCG strain, while expression of a mutated form of D4-DGI resulted in a higher number of granulomas (Kondoh et al., 2008). Dissemination of *M. marinum* during the end stage of tuberculosis in zebrafish might be facilitated by the strongly up-regulated expression of Rho GTPases.

Rab GTPases are essential regulators of vesicle trafficking, a process modulated by mycobacteria in order to prevent phagosome-lysosome fusion (Brumell and Scidmore, 2007). Maturation of phagosomes containing *M. tuberculosis* is blocked at the Rab5-positive stage (Via et al., 1997). The retainment of Rab5 facilitates the mycobacterial acquisition of iron within phagosomes through continued fusion with early endosomes (Kelley and Schorey, 2003). Mycobacterial phagosomes also retain Rab14 and Rab22 but do not acquire Rab7 that normally regulates late endocytic trafficking (Deretic et al., 1997; Kyei et al., 2006; Rink et al., 2005; Roberts et al., 2006; Via et al., 1997). Already at early time points after infection of zebrafish adults and embryos we observed a difference in the expression of a subset of Rab GTPases. Although Rab7 is commonly excluded from mycobacterial phagosomes, the expression of the zebrafish *rab7* gene was weakly induced during early stages of adult and embryonic infection and strongly at the end stage of infection. Interestingly, a group of nine small GTPase genes, including two members of the *rab5* family (*rab5al* and *zgc:110645*) showed significantly higher expression at the initial stage of *M. marinum* E11 infection compared with Mma20 infection (Table 1). These GTPases may therefore play a role in establishing the chronic disease phenotype.

4.6. WNT and TLR signaling

The expression of several genes involved in the canonical and non-canonical WNT-signaling pathways was affected during mycobacterial infection of adult and embryonic zebrafish, most notably at the end stages of infection with *M. marinum* strain E11 and Mma20. WNTs are secreted lipid-modified glycoproteins required for basic developmental processes, such as cell proliferation, cell fate specification, asymmetric cell division and axis formation. As a result abnormal WNT-signaling can induce pathological processes, such as carcinogenesis and chronic inflammation. In the last decade it has become clear that WNT-signaling plays a prominent role in the immune system as well, regulating effector T-cell development, regulatory T-cell activation and dendritic-cell maturation (Staal et al., 2008). Our transcriptome analysis showed that in mycobacterium-infected adult zebrafish mainly *wnt5a* transcription was up-regulated. As this was not observed during mycobacterium infection of embryos, *wnt5a* signaling may be linked to the adaptive rather than the innate immune response. In contrast, *wnt4a* expression was consistently up-regulated during all stages of mycbacterium infection in embryos, but down-regulated during the end stage of infection in adults. While Wnt4a has not been previously implicated in mycobacterial infections, the up-regulation of *wnt5a* in mycobacterium-infected adult zebrafish corroborates findings of Blumenthal et al. (2006), who reported up-regulation of *WNT5a* expression in human macrophages derived from *M. tuberculosis*-infected patients. Furthermore, Blumenthal et al. demonstrated that activation of TLR4 or TLR2 signaling cascades in human macrophages induced *WNT5a* expression (Blumenthal et al., 2006). These data are further supported by Pereira et al. (2008) who identified *WNT5a* transcript to be highly induced in human macrophages exposed to LPS and IFNγ and concluded that *WNT5a* is important in inflammatory macrophage signaling and that its expression is dependent on TLR signaling and NF-κB pathway activation. In addition, cross-talk between WNT5a and TLR4 was proposed to play a role in murine and human atherosclerotic lesions (Christman et al., 2008). In our analyses we also observed a clear effect on the transcription of zebrafish *tlr* genes and downstream components of the TLR signaling cascade, therefore also in zebrafish cross talk may exist between the evolutionary highly conserved TLR and WNT signaling pathways.

Expression of *tlr1* and *tlr2* was induced in infected zebrafish embryos and adults at multiple time points. Murine and human TLR1 and TLR2 have been implicated in the recognition of mycobacterial ligands (Hawn et al., 2007; Jo et al., 2007; Ryffel et al., 2005). Currently the role of TLRs as mediators of adaptive immunity in mycobacterial infections is under debate (Korbel et al., 2008; Reiling et al., 2008; Ryffel et al., 2005). Our observation that induction of *tlr1* and *tlr2* also occurs in the embryonic system is consistent with a role in innate immunity against mycobacterial infection. At the end stage of adult infections with the Mma20 and E11 strains we also observed induction of *tlr8b*, which is of interest since a recent study showed that *TLR8* is also up-regulated during the acute phase of disease in patients with pulmonary tuberculosis and that *TLR8* polymorphisms were associated with tuberculosis susceptibility (Davila et al., 2008). Furthermore, we found that *tlr9* and *tlr18*, which is closely related to *tlr1*, were specifically induced during the end stage of E11 infection, but not during any stage of Mma20 infection. Activation of murine TLR9 was shown to be required for maintenance of mycobacteria-elicited pulmonary granulomatous responses (Ito et al., 2007). The link between *tlr9* expression and the chronic disease causing E11 strain may suggest a conserved role in zebrafish. Finally, we observed that compared with E11 infection at 1 dpi, an infection with the acute Mma20 strain resulted in significantly higher *tlr5a* and *tlr5b* expression, the zebrafish orthologs of human *TLR5* (Stockhammer et al., 2009), and of *tlr21* and *tlr22*, encoding two fish-specific TLRs with unknown ligand specificity (Meijer et al., 2004). This suggests that Tlr5a and Tlr5b might respond to more signals than flagellin, the currently only known lig-

and (Stockhammer et al., 2009), and that inflammatory responses triggered by TLRs that are highly expressed during the initial phase of Mma20 infection may contribute to the acute disease phenotype.

5. Conclusions

In this study we have provided an extensive transcriptome data repository of mycobacterial infection stages in adult and embryonic zebrafish. We pinpointed and discussed gene groups that may determine the outcome of a mycobacterial infection being chronic with granuloma formation or acute with early lethality. These gene groups require functional testing and are important leads for follow up studies and validation in mammalian systems. It is clear from the data that many signaling cascades, including WNT and TLR pathways, are involved in determining the disease outcome and that balancing the transcriptional regulation is an important key for disease prognosis. A strong advantage of the zebrafish-mycobacterium model is the availability of an optically transparent and genetically tractable embryo system, in which the critical step of mycobacterium infection, i.e. granuloma formation, can be studied (Davis et al., 2002; Davis and Ramakrishnan, 2009). Interestingly, in a recent transcriptome profiling study of zebrafish embryos infected with a pathogenic or a non-pathogenic *S. typhimurium* strain infection we found a much stronger induction of the genes for immune-responsive transcription factors and inflammatory mediators than we observed during the time course of *M. marinum* infection (Stockhammer et al., 2009). This suggests that suppression of the host's innate inflammatory response contributes to immune evasion by mycobacteria in the embryonic system. Comparison of embryonic and adult infection allows dissecting the role of innate versus adaptive immunity in mycobacterial pathogenesis (Davis et al., 2002). Genes that respond similarly to infection in embryos and adult might determine if granuloma formation will occur and can conveniently be studied taking advantage of the genetic tools available for embryo experiments. Furthermore, a growing collection of zebrafish knockout and transgenic lines can be exploited for functional studies in adults. Recent studies in zebrafish have provided new insight into how pathogenic mycobacteria exploit the granuloma during the innate immune phase for local expansion and systemic dissemination (Davis and Ramakrishnan, 2009). Here we identified several genes of interest that have not been previously implicated in mycobacterial infections, but whose induction was common to infections in embryos and adults, suggestive of a function in the innate immune response. Examples include members of the Rhobtb (*rhobtb2a*), metalloproteinase (*adam8*), homeobox (*hhex*) and serine/threonine kinase (*melk*) families. By the identification of such common embryonic and adult-responsive genes and that of particular genes and gene groups that distinguish Mma20 and E11 infections we have obtained many useful directions for future research into the factors of the innate and adaptive immune system involved in tuberculosis.

Acknowledgments

We thank Frederike Hannes for technical assistance and Susan Wijting, Ulrike Nehrdich and Wim Schouten for assistance with infection experiments and fish care. This work was supported by the Centre for Medical Systems Biology, which is funded by the Netherlands Genomics Initiative (NGI), by the European Commission 6th framework project ZF-TOOLS (LSHG-CT-2006-037220) and by the SmartMix programme of the Netherlands Ministry of Economic Affairs and the Netherlands Ministry of Education, Culture and Science.

Appendix A. Supplementary data

Supplementary data associated with this article can be found, in the online version, at doi:10.1016/j.molimm.2009.03.024.

References

Basu, S., Pathak, S., Pathak, S.K., Bhattacharyya, A., Banerjee, A., Kundu, M., Basu, J., 2007. *Mycobacterium avium*-induced matrix metalloproteinase-9 expression occurs in a cyclooxygenase-2-dependent manner and involves phosphorylation- and acetylation-dependent chromatin modification. Cell. Microbiol. 9, 2804–2816.

Birkedal-Hansen, H., Moore, W.G., Bodden, M.K., Windsor, L.J., Birkedal-Hansen, B., DeCarlo, A., Engler, J.A., 1993. Matrix metalloproteinases: a review. Crit. Rev. Oral Biol. Med. 4, 197–250.

Bischof, J., Driever, W., 2004. Regulation of hhex expression in the yolk syncytial layer, the potential Nieuwkoop center homolog in zebrafish. Dev. Biol. 276, 552–562.

Blumenthal, A., Ehlers, S., Lauber, J., Buer, J., Lange, C., Goldmann, T., Heine, H., Brandt, E., Reiling, N., 2006. The Wingless homolog WNT5A and its receptor Frizzled-5 regulate inflammatory responses of human mononuclear cells induced by microbial stimulation. Blood 108, 965–973.

Blumenthal, A., Lauber, J., Hoffmann, R., Ernst, M., Keller, C., Buer, J., Ehlers, S., Reiling, N., 2005. Common and unique gene expression signatures of human macrophages in response to four strains of *Mycobacterium avium* that differ in their growth and persistence characteristics. Infect. Immun. 73, 3330–3341.

Boehm, U., Klamp, T., Groot, M., Howard, J.C., 1997. Cellular responses to interferon-gamma. Annu. Rev. Immunol. 15, 749–795.

Brumell, J.H., Scidmore, M.A., 2007. Manipulation of rab GTPase function by intracellular bacterial pathogens. Microbiol. Mol. Biol. Rev. 71, 636–652.

Caruso, A.M., Serbina, N., Klein, E., Triebold, K., Bloom, B.R., Flynn, J.L., 1999. Mice deficient in CD4 T cells have only transiently diminished levels of IFN-gamma, yet succumb to tuberculosis. J. Immunol. 162, 5407–5416.

Castilla, L.H., Perrat, P., Martinez, N.J., Landrette, S.F., Keys, R., Oikemus, S., Flanegan, J., Heilman, S., Garrett, L., Dutra, A., Anderson, S., Pihan, G.A., Wolff, L., Liu, P.P., 2004. Identification of genes that synergize with Cbfb-MYH11 in the pathogenesis of acute myeloid leukemia. Proc. Natl. Acad. Sci. U.S.A. 101, 4924–4929.

Chang, J.C., Wysocki, A., Tchou-Wong, K.M., Moskowitz, N., Zhang, Y., Rom, W.N., 1996. Effect of *Mycobacterium tuberculosis* and its components on macrophages and the release of matrix metalloproteinases. Thorax 51, 306–311.

Chopra, P., Koduri, H., Singh, R., Koul, A., Ghildiyal, M., Sharma, K., Tyagi, A.K., Singh, Y., 2004. Nucleoside diphosphate kinase of *Mycobacterium tuberculosis* acts as GTPase-activating protein for Rho-GTPases. FEBS Lett. 571, 212–216.

Christman 2nd, M.A., Goetz, D.J., Dickerson, E., McCall, K.D., Lewis, C.J., Benencia, F., Silver, M.J., Kohn, L.D., Malgor, R., 2008. Wnt5a is expressed in murine and human atherosclerotic lesions. Am. J. Physiol. Heart Circ. Physiol. 294, H2864–2870.

Clay, H., Davis, J.M., Beery, D., Huttenlocher, A., Lyons, S.E., Ramakrishnan, L., 2007. Dichotomous role of the macrophage in early *Mycobacterium marinum* infection of the zebrafish. Cell Host Microbe 2, 29–39.

Coussens, P.M., Colvin, C.J., Rosa, G.J., Perez Laspiur, J., Elftman, M.D., 2003. Evidence for a novel gene expression program in peripheral blood mononuclear cells from *Mycobacterium avium* subsp. paratuberculosis-infected cattle. Infect. Immun. 71, 6487–6498.

Davidson, A.J., Zon, L.I., 2004. The 'definitive' (and 'primitive') guide to zebrafish hematopoiesis. Oncogene 23, 7233–7246.

Davila, S., Hibberd, M.L., Hari Dass, R., Wong, H.E., Sahiratmadja, E., Bonnard, C., Alisjahbana, B., Szeszko, J.S., Balabanova, Y., Drobniewski, F., van Crevel, R., van de Vosse, E., Nejentsev, S., Ottenhoff, T.H., Seielstad, M., 2008. Genetic association and expression studies indicate a role of toll-like receptor 8 in pulmonary tuberculosis. PLoS Genet. 4, e1000218.

Davis, J.M., Clay, H., Lewis, J.L., Ghori, N., Herbomel, P., Ramakrishnan, L., 2002. Real-time visualization of mycobacterium-macrophage interactions leading to initiation of granuloma formation in zebrafish embryos. Immunity 17, 693–702.

Davis, J.M., Ramakrishnan, L., 2009. The role of the granuloma in expansion and dissemination of early tuberculous infection. Cell 136, 37–49.

Dennis Jr., G., Sherman, B.T., Hosack, D.A., Yang, J., Gao, W., Lane, H.C., Lempicki, R.A., 2003. DAVID: database for annotation, visualization, and integrated discovery. Genome Biol. 4, P3.

Deretic, V., Via, L.E., Fratti, R.A., Deretic, D., 1997. Mycobacterial phagosome maturation, rab proteins, and intracellular trafficking. Electrophoresis 18, 2542–2547.

Drew, P.D., Franzoso, G., Becker, K.G., Bours, V., Carlson, L.M., Siebenlist, U., Ozato, K., 1995. NF kappa B and interferon regulatory factor 1 physically interact and synergistically induce major histocompatibility class I gene expression. J. Interferon Cytokine Res. 15, 1037–1045.

Elkington, P.T., Green, J.A., Emerson, J.E., Lopez-Pascua, L.D., Boyle, J.J., O'Kane, C.M., Friedland, J.S., 2007. Synergistic up-regulation of epithelial cell matrix metalloproteinase-9 secretion in tuberculosis. Am. J. Respir. Cell. Mol. Biol. 37, 431–437.

Fernandez de Mera, I.G., Perez de la Lastra, J.M., Ayoubi, P., Naranjo, V., Kocan, K.M., Gortazar, C., de la Fuente, J., 2008. Differential expression of inflammatory and immune response genes in mesenteric lymph nodes of Iberian red deer (*Cervus elaphus hispanicus*) naturally infected with *Mycobacterium bovis*. Dev. Comp. Immunol. 32, 85–91.

Flynn, J.L., Chan, J., 2001. Immunology of tuberculosis. Annu. Rev. Immunol. 19, 93–129.

Flynn, J.L., Chan, J., 2003. Immune evasion by *Mycobacterium tuberculosis*: living with the enemy. Curr. Opin. Immunol. 15, 450–455.
Fratti, R.A., Vergne, I., Chua, J., Skidmore, J., Deretic, V., 2000. Regulators of membrane trafficking and *Mycobacterium tuberculosis* phagosome maturation block. Electrophoresis 21, 3378–3385.
Goetzl, E.J., Banda, M.J., Leppert, D., 1996. Matrix metalloproteinases in immunity. J. Immunol. 156, 1–4.
Gonzalez-Avila, G., Sandoval, C., Herrera, M.T., Ruiz, V., Sommer, B., Sada, E., Ramos, C., Sarabia, M.C., 2009. *Mycobacterium tuberculosis* effects on fibroblast collagen metabolism. Respiration 77, 195–202.
Goodbourn, S., Didcock, L., Randall, R.E., 2000. Interferons: cell signalling, immune modulation, antiviral response and virus countermeasures. J. Gen. Virol. 81, 2341–2364.
Gordon, S., Keshav, S., Stein, M., 1994. BCG-induced granuloma formation in murine tissues. Immunobiology 191, 369–377.
Grotzke, J.E., Lewinsohn, D.M., 2005. Role of CD8+ T lymphocytes in control of *Mycobacterium tuberculosis* infection. Microbes Infect. 7, 776–788.
Hawn, T.R., Misch, E.A., Dunstan, S.J., Thwaites, G.E., Lan, N.T., Quy, H.T., Chau, T.T., Rodrigues, S., Nachman, A., Janer, M., Hien, T.T., Farrar, J.J., Aderem, A., 2007. A common human TLR1 polymorphism regulates the innate immune response to lipopeptides. Eur. J. Immunol. 37, 2280–2289.
Herbomel, P., Thisse, B., Thisse, C., 1999. Ontogeny and behaviour of early macrophages in the zebrafish embryo. Development 126, 3735–3745.
Herbomel, P., Thisse, B., Thisse, C., 2001. Zebrafish early macrophages colonize cephalic mesenchyme and developing brain, retina, and epidermis through a M-CSF receptor-dependent invasive process. Dev. Biol. 238, 274–288.
Ito, T., Schaller, M., Hogaboam, C.M., Standiford, T.J., Chensue, S.W., Kunkel, S.L., 2007. TLR9 activation is a key event for the maintenance of a mycobacterial antigen-elicited pulmonary granulomatous response. Eur. J. Immunol. 37, 2847–2855.
Jenner, R.G., Young, R.A., 2005. Insights into host responses against pathogens from transcriptional profiling. Nat. Rev. Microbiol. 3, 281–294.
Jo, E.K., Yang, C.S., Choi, C.H., Harding, C.V., 2007. Intracellular signalling cascades regulating innate immune responses to Mycobacteria: branching out from Toll-like receptors. Cell. Microbiol. 9, 1087–1098.
Kaul, D., 2008. Coronin-1A epigenomics governs mycobacterial persistence in tuberculosis. FEMS Microbiol. Lett. 278, 10–14.
Kelley, V.A., Schorey, J.S., 2003. Mycobacterium's arrest of phagosome maturation in macrophages requires Rab5 activity and accessibility to iron. Mol. Biol. Cell. 14, 3366–3377.
Kimmel, C.B., Ballard, W.W., Kimmel, S.R., Ullmann, B., Schilling, T.F., 1995. Stages of embryonic development of the zebrafish. Dev. Dyn. 203, 253–310.
Kondoh, K., Nakata, Y., Yamaoka, T., Itakura, M., Hayashi, M., Yamada, K., Hata, J., Yamada, T., 2008. Altered cellular immunity in transgenic mice with T cell-specific expression of human D4-guanine diphosphate-dissociation inhibitor (D4-GDI). Int. Immunol. 20, 1299–1311.
Korbel, D.S., Schneider, B.E., Schaible, U.E., 2008. Innate immunity in tuberculosis: myths and truth. Microbes Infect. 10, 995–1004.
Kotekar, A.S., Weissman, J.D., Gegonne, A., Cohen, H., Singer, D.S., 2008. Histone modifications, but not nucleosomal positioning, correlate with major histocompatibility complex class I promoter activity in different tissues in vivo. Mol. Cell. Biol. 28, 7323–7336.
Krens, S.F., Corredor-Adámez, M., He, S., Snaar-Jagalska, B.E., Spaink, H.P., 2008. ERK1 and ERK2 MAPK are key regulators of distinct gene sets in zebrafish embryogenesis. BMC Genomics 28, 196.
Kyei, G.B., Vergne, I., Chua, J., Roberts, E., Harris, J., Junutula, J.R., Deretic, V., 2006. Rab14 is critical for maintenance of *Mycobacterium tuberculosis* phagosome maturation arrest. EMBO J. 25, 5250–5259.
Lam, S.H., Chua, H.L., Gong, Z., Lam, T.J., Sin, Y.M., 2004. Development and maturation of the immune system in zebrafish, *Danio rerio*: a gene expression profiling, *in situ* hybridization and immunological study. Dev. Comp. Immunol. 28, 9–28.
Landrette, S.F., Kuo, Y.H., Hensen, K., Barjesteh van Waalwijk van Doorn-Khosrovani, S., Perrat, P.N., Van de Ven, W.J., Delwel, R., Castilla, L.H., 2005. Plag1 and Plagl2 are oncogenes that induce acute myeloid leukemia in cooperation with Cbfb-MYH11. Blood 105, 2900–2907.
Lemonnier, M., Landraud, L., Lemichez, E., 2007. Rho GTPase-activating bacterial toxins: from bacterial virulence regulation to eukaryotic cell biology. FEMS Microbiol. Rev. 31, 515–534.
Lerm, M., Schmidt, G., Aktories, K., 2000. Bacterial protein toxins targeting rho GTPases. FEMS Microbiol. Lett. 188, 1–6.
Lesley, R., Ramakrishnan, L., 2008. Insights into early mycobacterial pathogenesis from the zebrafish. Curr. Opin. Microbiol. 11, 277–283.
Liao, W., Ho, C.Y., Yan, Y.L., Postlethwait, J., Stainier, D.Y., 2000. Hhex and scl function in parallel to regulate early endothelial and blood differentiation in zebrafish. Development 127, 4303–4313.
Manabe, Y.C., Bishai, W.R., 2000. Latent *Mycobacterium tuberculosis*-persistence, patience, and winning by waiting. Nat. Med. 6, 1327–1329.
Marquis, J.F., Nantel, A., LaCourse, R., Ryan, L., North, R.J., Gros, P., 2008. Fibrotic response as a distinguishing feature of resistance and susceptibility to pulmonary infection with *Mycobacterium tuberculosis* in mice. Infect. Immun. 76, 78–88.
Martin, S.A., Zou, J., Houlihan, D.F., Secombes, C.J., 2007. Directional responses following recombinant cytokine stimulation of rainbow trout (*Oncorhynchus mykiss*) RTS-11 macrophage cells as revealed by transcriptome profiling. BMC Genomics 8, 150.
Meijer, A.H., Gabby Krens, S.F., Medina Rodriguez, I.A., He, S., Bitter, W., Ewa Snaar-Jagalska, B., Spaink, H.P., 2004. Expression analysis of the Toll-like receptor and TIR domain adaptor families of zebrafish. Mol. Immunol. 40, 773–783.
Meijer, A.H., Verbeek, F.J., Salas-Vidal, E., Corredor-Adamez, M., Bussman, J., van der Sar, A.M., Otto, G.W., Geisler, R., Spaink, H.P., 2005. Transcriptome profiling of adult zebrafish at the late stage of chronic tuberculosis due to *Mycobacterium marinum* infection. Mol. Immunol. 42, 1185–1203.
Muller, I., Cobbold, S.P., Waldmann, H., Kaufmann, S.H., 1987. Impaired resistance to *Mycobacterium tuberculosis* infection after selective in vivo depletion of L3T4+ and Lyt-2+ T cells. Infect. Immun. 55, 2037–2041.
Murayama, E., Kissa, K., Zapata, A., Mordelet, E., Briolat, V., Lin, H.F., Handin, R.I., Herbomel, P., 2006. Tracing hematopoietic precursor migration to successive hematopoietic organs during zebrafish development. Immunity 25, 963–975.
Naranjo, V., Hofle, U., Vicente, J., Martin, M.P., Ruiz-Fons, F., Gortazar, C., Kocan, K.M., de la Fuente, J., 2006. Genes differentially expressed in oropharyngeal tonsils and mandibular lymph nodes of tuberculous and nontuberculous European wild boars naturally exposed to *Mycobacterium bovis*. FEMS Immunol. Med. Microbiol. 46, 298–312.
Orme, I.M., Collins, F.M., 1983. Protection against *Mycobacterium tuberculosis* infection by adoptive immunotherapy. Requirement for T cell-deficient recipients. J. Exp. Med. 158, 74–83.
Parks, W.C., Wilson, C.L., Lopez-Boado, Y.S., 2004. Matrix metalloproteinases as modulators of inflammation and innate immunity. Nat. Rev. Immunol. 4, 617–629.
Pennini, M.E., Pai, R.K., Schultz, D.C., Boom, W.H., Harding, C.V., 2006. *Mycobacterium tuberculosis* 19-kDa lipoprotein inhibits IFN-gamma-induced chromatin remodeling of MHC2TA by TLR2 and MAPK signaling. J. Immunol. 176, 4323–4330.
Pereira, C., Schaer, D.J., Bachli, E.B., Kurrer, M.O., Schoedon, G., 2008. Wnt5A/CaMKII signaling contributes to the inflammatory response of macrophages and is a target for the antiinflammatory action of activated protein C and interleukin-10. Arterioscler. Thromb. Vasc. Biol. 28, 504–510.
Quiding-Jarbrink, M., Smith, D.A., Bancroft, G.J., 2001. Production of matrix metalloproteinases in response to mycobacterial infection. Infect. Immun. 69, 5661–5670.
Raju, B., Hoshino, Y., Belitskaya-Levy, I., Dawson, R., Ress, S., Gold, J.A., Condos, R., Pine, R., Brown, S., Nolan, A., Rom, W.N., Weiden, M.D., 2008. Gene expression profiles of bronchoalveolar cells in pulmonary TB. Tuberculosis (Edinburgh) 88, 39–51.
Reiling, N., Ehlers, S., Holscher, C., 2008. MyDths and un-TOLLed truths: sensor, instructive and effector immunity to tuberculosis. Immunol. Lett. 116, 15–23.
Rink, J., Ghigo, E., Kalaidzidis, Y., Zerial, M., 2005. Rab conversion as a mechanism of progression from early to late endosomes. Cell 122, 735–749.
Roberts, E.A., Chua, J., Kyei, G.B., Deretic, V., 2006. Higher order Rab programming in phagolysosome biogenesis. J. Cell Biol. 174, 923–929.
Russell, D.G., 2001. *Mycobacterium tuberculosis*: here today, and here tomorrow. Nat. Rev. Mol. Cell. Biol. 2, 569–577.
Ryffel, B., Fremond, C., Jacobs, M., Parida, S., Botha, T., Schnyder, B., Quesniaux, V., 2005. Innate immunity to mycobacterial infection in mice: critical role for toll-like receptors. Tuberculosis (Edinburgh) 85, 395–405.
Salas-Vidal, E., Meijer, A.H., Cheng, X., Spaink, H.P., 2005. Genomic annotation and expression analysis of the zebrafish Rho small GTPase family during development and bacterial infection. Genomics 86, 25–37.
Sangari, F.J., Goodman, J., Bermudez, L.E., 2000. *Mycobacterium avium* enters intestinal epithelial cells through the apical membrane, but not by the basolateral surface, activates small GTPase Rho and, once within epithelial cells, expresses an invasive phenotype. Cell. Microbiol. 2, 561–568.
Schonbeck, U., Mach, F., Libby, P., 1998. Generation of biologically active IL-1 beta by matrix metalloproteinases: a novel caspase-1-independent pathway of IL-1 beta processing. J. Immunol. 161, 3340–3346.
Serbina, N.V., Flynn, J.L., 1999. Early emergence of CD8(+) T cells primed for production of type 1 cytokines in the lungs of *Mycobacterium tuberculosis*-infected mice. Infect. Immun. 67, 3980–3988.
Sheen, P., O'Kane, C.M., Chaudhary, K., Tovar, M., Santillan, C., Sosa, J., Caviedes, L., Gilman, R.H., Stamp, G., Friedland, J.S., 2009. High MMP-9 activity characterises pleural tuberculosis correlating with granuloma formation. Eur. Respir. J. 33, 134–141.
Staal, F.J., Luis, T.C., Tiemessen, M.M., 2008. WNT signalling in the immune system: WNT is spreading its wings. Nat. Rev. Immunol. 8, 581–593.
Stamm, L.M., Morisaki, J.H., Gao, L.Y., Jeng, R.L., McDonald, K.L., Roth, R., Takeshita, S., Heuser, J., Welch, M.D., Brown, E.J., 2003. *Mycobacterium marinum* escapes from phagosomes and is propelled by actin-based motility. J. Exp. Med. 198, 1361–1368.
Stewart, G.R., Robertson, B.D., Young, D.B., 2003. Tuberculosis: a problem with persistence. Nat. Rev. Microbiol. 1, 97–105.
Stockhammer, O.W., Zakrzewska, A., Hegedus, Z., Spaink, H.P., Meijer, A.H., 2009. Transcriptome profiling and functional analyses of the zebrafish embryonic innate immune response to Salmonella infection. J. Immunol. 182, 5641–5653.
Swaim, L.E., Connolly, L.E., Volkman, H.E., Humbert, O., Born, D.E., Ramakrishnan, L., 2006. *Mycobacterium marinum* infection of adult zebrafish causes caseating granulomatous tuberculosis and is moderated by adaptive immunity. Infect. Immun. 74, 6108–6117.
Taylor, J.L., Hattle, J.M., Dreitz, S.A., Troudt, J.M., Izzo, L.S., Basaraba, R.J., Orme, I.M., Matrisian, L.M., Izzo, A.A., 2006. Role for matrix metalloproteinase 9 in granuloma formation during pulmonary *Mycobacterium tuberculosis* infection. Infect. Immun. 74, 6135–6144.

Teles, R.M., Antunes, S.L., Jardim, M.R., Oliveira, A.L., Nery, J.A., Sales, A.M., Sampaio, E.P., Shubayev, V., Sarno, E.N., 2007. Expression of metalloproteinases (MMP-2, MMP-9, and TACE) and TNF-alpha in the nerves of leprosy patients. J. Peripher. Nerv. Syst. 12, 195–204.

van der Sar, A.M., Abdallah, A.M., Sparrius, M., Reinders, E., Vandenbroucke-Grauls, C.M., Bitter, W., 2004. *Mycobacterium marinum* strains can be divided into two distinct types based on genetic diversity and virulence. Infect. Immun. 72, 6306–6312.

van der Wel, N., Hava, D., Houben, D., Fluitsma, D., van Zon, M., Pierson, J., Brenner, M., Peters, P.J., 2007. *M. tuberculosis* and *M. leprae* translocate from the phagolysosome to the cytosol in myeloid cells. Cell 129, 1287–1298.

Via, L.E., Deretic, D., Ulmer, R.J., Hibler, N.S., Huber, L.A., Deretic, V., 1997. Arrest of mycobacterial phagosome maturation is caused by a block in vesicle fusion between stages controlled by rab5 and rab7. J. Biol. Chem. 272, 13326–13331.

Wang, T., Lafuse, W.P., Takeda, K., Akira, S., Zwilling, B.S., 2002. Rapid chromatin remodeling of Toll-like receptor 2 promoter during infection of macrophages with *Mycobacterium avium*. J. Immunol. 169, 795–801.

Wang, Y., Curry, H.M., Zwilling, B.S., Lafuse, W.P., 2005. Mycobacteria inhibition of IFN-gamma induced HLA-DR gene expression by up-regulating histone deacetylation at the promoter region in human THP-1 monocytic cells. J. Immunol. 174, 5687–5694.

Weiss, D.J., Evanson, O.A., Deng, M., Abrahamsen, M.S., 2004. Sequential patterns of gene expression by bovine monocyte-derived macrophages associated with ingestion of mycobacterial organisms. Microb. Pathog. 37, 215–224.

Willett, C.E., Cortes, A., Zuasti, A., Zapata, A.G., 1999. Early hematopoiesis and developing lymphoid organs in the zebrafish. Dev. Dyn. 214, 323–336.

Wolfsberg, T.G., Primakoff, P., Myles, D.G., White, J.M., 1995. ADAM, a novel family of membrane proteins containing A disintegrin and metalloprotease domain: multipotential functions in cell–cell and cell–matrix interactions. J. Cell Biol. 131, 275–278.

Yamamoto, S., Higuchi, Y., Yoshiyama, K., Shimizu, E., Kataoka, M., Hijiya, N., Matsuura, K., 1999. ADAM family proteins in the immune system. Immunol. Today 20, 278–284.

Young, N.D., Cooper, G.A., Nowak, B.F., Koop, B.F., Morrison, R.N., 2008. Coordinated down-regulation of the antigen processing machinery in the gills of amoebic gill disease-affected Atlantic salmon (*Salmo salar L.*). Mol. Immunol. 45, 2581–2597.